The geochemical composition of serpentinites in the Mesoarchaean Tartoq Group, SW Greenland: Harzburgitic cumulates or melt-modified mantle?

Kristoffer Szilas [a, b, *], Vincent J. Van Hinsberg [c], Robert A. Creaser [d], Alex F.M. Kisters [e]

[a] Lamont-Doherty Earth Observatory, Palisades, NY 10964-8000, USA
[b] Natural History Museum of Denmark, Copenhagen 1350, Denmark
[c] Department of Earth & Planetary Sciences, McGill University, Quebec, Canada
[d] Department of Earth & Atmospheric Sciences, University of Alberta, Edmonton, Canada
[e] Department of Earth Sciences, Stellenbosch University, Matieland 7602, South Africa

* Corresponding author K. Szilas
E-mail: kszilas@ldeo.columbia.edu

Abstract

Large slivers and enclaves (up to 100 x 2000 meters) of serpentinites form tectonic imbricates within mafic supracrustal rocks of the Mesoarchaean Tartoq Group in SW Greenland. In this study we present new bulk-rock major, trace and platinum-group element data, and preliminary Re-Os isotope data for these serpentinites. Additionally, we present in situ major and trace element data for chromite and magnetite.

Bulk-serpentinite major and trace element compositions allow us to rule out komatiitic, picritic, boninitic or residual mantle origins. Rather, the fractionated platinum-group patterns for the Tartoq Group serpentinites suggest a cumulate origin. The bulk-rock Re-Os isotope data shows Re-depletion ages (T_{RD}) of ca. 2300, 2800 and 2950 Ma for the three analysed samples. These ages are younger than the 2986 ± 4 Ma minimum age of the Tartoq Group, and suggest disturbance of the Re-Os system during metamorphism or post-magmatic metasomatic events. Late resetting and metamorphic overprinting is in agreement with oxide mineral compositions, which are not primary

as indicated by negligible Mg and Al contents and elevated Fe^{3+}# (>55). Although the major and trace element data do not provide conclusive evidence for the petrogenesis of these Mesoarchaean serpentinites, we observe remarkable similarities with ultramafic rocks associated with the lower crustal cumulates. In particular, ultramafic cumulates of the Kohistan and Talkeetna island arc sections are compositionally comparable, if we allow for slight loss of MgO and addition of SiO_2 during early alteration, serpentinisation and metamorphism. Based on these similarities, we propose an arc origin for the Tartoq Group serpentinites. Previous geochemical and structural studies of the enclosing Tartoq Group supracrustal rocks also point to formation in a subduction zone geodynamic setting. This suggests that this assemblage of imbricated mafic to ultramafic rocks and minor sediments represents a Mesoarchaean arc-related ophiolite.

Keywords: Archaean; Ultramafic cumulates; Metamorphic spinel; Platinum-group elements; Olivine fractionation

1. Introduction

Serpentinites, especially those of Archaean age, are commonly difficult to interpret in terms of their petrogenesis, because relics of their primary mineralogy are rarely preserved and hydration is assumed to have modified their bulk-rock compositions (e.g., Dechamps et al., 2013; Matchesi et al., 2013). Here, we present new geochemical data for serpentinites of Mesoarchaean age from the Tartoq Group of SW Greenland, and show that these ultramafic rocks preserve sufficient geochemical characteristics to reconstruct their protoliths and their likely geotectonic setting.

Detailed information on the structural geology and the geochemical composition of the Mesoarchaean Tartoq Group has recently become available (Kisters et al., 2012; Szilas et al., 2013a). Nevertheless, the petrogenesis of the large serpentinite bodies (up to 100 x 2000 meters)

that are associated with the supracrustal rocks is poorly constrained at present, and several possible origins can be imagined for these ultramafic rocks, e.g., 1) picritic/komatiitic lava flows, 2) ultramafic cumulates, 3) mantle residues, 4) melt-mantle reaction products, or 5) tectonised subcontinental mantle.

The structural analysis of Kisters et al. (2012) concluded that the fabrics of the Tartoq Group are consistent with burial and subsequent return flow during subduction–accretion along an obliquely convergent margin. This interpretation is in agreement with the geochemical signatures of the mafic rocks, which Szilas et al. (2013a) interpreted as being indicative of a fore-arc or back-arc geodynamic setting. These authors further argued that the Tartoq Group represents a dismembered arc-related ophiolite (cf., Dilek, 2003), and the associated serpentinites were inferred to represent the lower crustal ultramafic cumulate/mantle portion of this island arc-related oceanic crust section. Here, we test this hypothesis in a detailed study of bulk-rock major, trace and platinum-group element data from these serpentinites, which we compare with published data of ultramafic rocks from a broad range of geological settings.

2. Regional geology

The Tartoq Group supracrustal rocks are located within Archaean orthogneisses near the southern margin of the North Atlantic craton (see Windley and Garde, 2009). The Tartoq Group comprises several km-sized, tectonic and subsequently intruded and brecciated mafic slivers and enclaves along the Sermiligaarsuk Fjord (**Fig. 1**). Early work suggested that the Tartoq Group was deposited onto Archaean basement (Higgins and Bondesen, 1966; Higgins, 1968), whereas later studies re-interpreted the mafic volcanic sequence as relics of oceanic crust with associated volcanogenic massive sulfide deposits (e.g., Appel and Secher, 1984; Petersen, 1992; Evans and

King, 1993). It is now well-established that intrusive granitoid sheets of the tonalite-trondhjemite-granodiorite (TTG) suite cut the Tartoq Group and that the supracrustal rocks predate all of the regional orthogneisses. These TTG intrusives yield U-Pb zircon minimum ages of 2944 ± 7 Ma (Nutman and Kalsbeek, 1994) and 2986 ± 4 Ma (Szilas et al., 2013a). The mafic supracrustal rocks themselves yield a Lu-Hf errorchron age of 3189 ± 65 Ma, consistent with the Mesoarchaean minimum age from TTG sheets (Szilas et al., 2013a). Most of the supracrustal slivers display both fault-bounded and intrusive contacts with the TTG gneisses, which have been interpreted to reflect burial and exhumation of the supracrustal rocks along a convergent margin (Kisters et al., 2012). This is consistent with the overall geochemical characteristics of the Tartoq Group mafic tholeiitic rocks, which indicates an island arc-related affinity (Szilas et al., 2013a). The mafic supracrustal rocks record metamorphic conditions ranging from greenschist to lower granulite facies (Van Hinsberg et al., 2010; Kisters et al., 2012). Large parts of the Tartoq Group have undergone variable degrees of retrogression and hydrothermal overprint (Van Hinsberg et al., 2010). Early mylonitic and late cataclastic fabrics are commonly observed in carbonated high strain zones that show evidence of extensive hydrothermal fluid flow and which are associated with Au occurrences (King, 1985; Petersen, 1992; Evans and King, 1993). These high-strain zones are usually marked by mylonitic felsic schists from which detrital zircon with ages as young as 2824 ± 6 Ma have been extracted (Nutman et al., 2004). This age represents the minimum age constraint for the imbrication of the Tartoq Group with younger TTG gneisses. The late thrusting and carbonate alteration postdates the TTG formation, but predates the ca. 1800 Ma Ketilidian orogen based on the structural geology (Van Hinsberg et al., 2010; Kisters et al., 2011, 2012).

Berthelsen and Henriksen (1975) suggested that sheet-like serpentinites in the Bikuben sliver (**Fig. 1**) could be intrusive into the Tartoq Group and that they may represent ultramafic sills or dykes. However, Szilas et al. (2013a) noted that that there are no crosscutting relationships to

support this claim. Instead the steeper-dipping fabric of some talc-schists, relative to the surrounding mafic amphibolites and greenschists likely resulted from localised strain in the relatively incompetent talc schists. Moreover, talc fabrics commonly postdate the foliation in the enclosing schists and gneisses. Thus, the highly sheared contacts of the serpentinites provide little information about their original contact relationships or protoliths. Furthermore, the geochemical compositions of the serpentinites are not compatible with any known ultramafic magmas (**Section 6.2**). Nevertheless, it should be noted that the serpentinites invariably occur in areas with strong deformation, and are commonly in contact with TTG gneiss thrust sheets. This suggests at least a local structural control on their position within the Tartoq Group stratigraphy.

Pegmatites and granites of currently unknown ages intrude the Tartoq Group, as well as the TTG orthogneisses. These are themselves cut by several generations of post-tectonic mafic dykes of likely Mesozoic age (Higgins, 1990). The Palaeoproterozoic Ketilidian supracrustal rocks unconformably overly the Tartoq Group and the Archaean orthogneiss terrane to the east (Higgins and Bondesen, 1966; Berthelsen and Henriksen, 1975).

3. Samples and petrography

Serpentinite samples presented in this study were collected from five different mafic slivers in the Tartoq Group (**Fig. 1**). The serpentinites generally crop out as elongate bodies that can be traced for tens of metres to several kilometres and have thicknesses up to 100 meters (**Fig. 2**). They always have a margin consisting of talc–carbonate–magnetite schist, but the thickness of this rind varies considerably (Fig. 2d). For example, at Iterlak most outcrops are completely hydrated to carbonated talc schists, whereas at Bikuben talc schists form only thin rinds of a few cm, thereby mimicking the extent of retrogression of their mafic host rocks. The serpentinites consist mainly of serpentine

and disseminated magnetite/chromite, although some samples also contain magnetite segregations and veins. In one locality (Amitsuarsua), chromite forms a boxwork or mesh that outlines relict mineral textures (**Fig. 3a**). This serpentinite sliver is the least deformed ultramafic body observed in the Tartoq Group, and, together with its metamorphic grade, low-amphibolites facies (van Hinsberg et al., 2010), is the most likely locality to preserve primary textures. Szilas et al. (2013a) interpreted this texture as that of a primary olivine-rich cumulate or mantle rock. In contrast, the magnetite veins in several higher grade metamorphic grade serpentinites in the Bikuben sliver (**Fig. 3b**), which give the rock a spinifex-like texture, are resulting from later segregation of magnetite, likely during growth of metamorphic amphibole. These magnetites lack chromite cores and are texturally distinct. Transitions from serpentinite to the enclosing talc-schists are abrupt and no gradual change in mineralogy is observed. Although this could be a reaction front, the complete absence of carbonate minerals in the serpentinites, and the difference in foliation generation between serpentinite and talc-schists lead us to conclude that the ultramafic rocks have been subjected to two metasomatic events: 1) initial serpentinisation of primary minerals; and 2) later hydration and carbonation to form the talc-schist rinds.

The serpentinite bodies either occur close to the sheared contacts between the supracrustal rocks and the surrounding TTG gneisses or in the central parts of mafic slivers (**Fig. 2**). In the latter case, the serpentinites are spatially closely associated with internal shear zones that led to the structural assembly of larger mafic slivers. For example, in the Amitsuarsua sliver a ca. 50 × 200 m serpentinite body is completely enveloped by sheared greenschists that form part of the central, several tens of meter wide strike-slip zone within the supracrustal belt (Kisters et al., 2012). In the eastern part of Iterlak the serpentinites are strongly sheared into a thin linear belt on the thrust plane (**Fig. 2**). These rocks can be traced into a unit of sheared and finely laminated (mm-scale) magnetite-amphibole rocks that have the appearance of banded iron formation (BIF). This locality

was described as BIF sensu stricto by Appel (1984), but due to the above-mentioned field observations, we re-interpret it as a metasomatic lithology. Such strongly metasomatised rocks are not included in the present study.

4. Methods

We have acquired major and trace element data by ICP methods from ACMELabs, Vancouver. Platinum-group element data were obtained at Université du Québec à Chicoutimi by NiS-FA pre-concentration followed by MC-ICP-MS measurement (Savard et al., 2010). Electron microprobe and LA-ICP-MS trace element analysis of oxide minerals was conducted at McGill University, Montreal. Re-Os isotope analysis was completed at the University of Alberta by carius tube digestion and N-TIMS measurement. The reader is referred to the online **Appendix A** for a detailed description of the analytical procedures. We present additional geochemical plots and diagrams in **Appendix B** and give the references to these figures the prefix 'B'. All geochemical diagrams were made in the GCDKit freeware program of Janosek et al. (2006).

5. Results

5.1. Bulk-rock major and trace element data

We have acquired major and trace element data for six serpentinite samples (**Supplementary Table 1**), which supplement the fifteen samples that were previously published in Szilas et al. (2013a) and the following presentation of the Tartoq Group serpentinites is based on the combined dataset. These data are fully comparable, because the new analyses were performed at the same

laboratory in a batch that immediately followed the previously published data. All data have been normalised to a volatile free composition. Loss on ignition (LOI) from dehydration and decarbonation range from 9.4 to 23.6 wt.% (median value of 12.2 wt.%). We have divided the serpentinites into a low- and high-Ir group, as explained in **Section 5.2.** However, these two groups do not appear to have significant major or trace element differences and are thus described together in the following section.

The Tartoq Group serpentinites (n = 21) are MgO-rich (34.94-41.95 wt.%) and have variable Al_2O_3 (0.13-5.51 wt.%), CaO (0.02-2.97 wt.%) and TiO_2 (0.00-0.26 wt.%). They have FeOt of 9.50-17.27 wt.% and SiO_2 ranges between 40.61 and 49.70 wt.%, as seen in **Figure 4**. Na_2O, K_2O and P_2O_5 are virtually absent in these rocks. Chromium concentrations are between 452 and 5337 ppm and Ni ranges between 229 and 3110 ppm (**Fig. 4**). Many of the incompatible trace elements are present in abundances that are below the analytical detection limits in our data set. This is the case for Th, Ta, U and W and to some degree for Ba, Cs, Hf and Nd. The serpentinites have variable chondrite-normalised rare earth element (REE) patterns with $(La/Sm)_{CN}$ from 0.70 to 3.64 and Eu/Eu* from 0.41 to 2.00 (**Fig. B1**). Their primitive mantle-normalised trace element patterns are relatively flat with large positive anomalies for Pb, large negative anomalies for Sr (**Fig. 5**).

We have calculated the normative mineralogy of the serpentinites following the procedure of Kelemen et al. (1992, 1998) in order to estimate the mineralogy of their protoliths (**Supplementary Table 1**). Our calculations suggest that these rocks were originally harzburgites (**Fig. B2**) with olivine Mg# between 73 and 84. However, we point out that there are large uncertainties in these estimates, and the Mg# in particular, resulting from obvious post-magmatic disturbance to these ultramafic rocks during serpentinisation and metamorphism (see **Section 6.1**).

5.2. Platinum-group element data

We have acquired platinum-group element (PGE) data for all of the 21 serpentinite samples from the Tartoq Group. This data can be found in **Supplementary Table 2**. We present the PGEs normalised to the chondrite abundances of Fisher-Gödde et al. (2010) and have added Au to complete the incompatible part of the pattern.

In general, two different types of PGE patterns can be distinguished in the Tartoq Group serpentinites (**Fig. 6**): 1) high-Ir group and 2) low-Ir group, which can be differentiated by having values of above or below 1.5 ppb Ir, respectively (the detection limit of Ir is 0.025 ppb and the 1σ-uncertainty is 0.07 ppb).

We found that the textures of the high-Ir group are commonly of the boxwork/mesh type, whereas the low-Ir group samples are generally of the magnetite-veined type. However, given that these two groups may simply represent a continuum of two end-members, this classification may be rather arbitrary.

The high-Ir group is characterised by relatively high Os and Ir abundances (>2.0 and >1.79 ppb, respectively) and by having negative slopes from Os to Pt. Whereas the serpentinites of the low-Ir group have distinctly positive Ru anomalies with the exception of sample 510777, which has the lowest Ru value of all samples (1.06 ppb). Almost all of the samples display negative Pt anomalies.

5.3. Electron microprobe data

Major element data for oxide minerals in the serpentinite samples show that these are spinels, with most of their compositional variation between the chromite and magnetite end-members (**Supplementary Table 3**). The highest chromite contents, with up to 85% chromite component, were observed in the cores of large oxide grains and in the least deformed samples. No high-Cr

oxides were observed among small grains or in the minor oxide segregations. One sample from Amitsuarsua (509632) also contained ilmenite, which was intergrown with low-Cr magnetite. Overall the Tartoq Group chromites have very low Mg# (<2), high Cr# (>74) and high Fe^{3+}# (>55) as shown in **Figures B3-B4**.

5.4. In situ spinel trace element data

Trace element concentrations were determined for a subset of oxide grains analysed by electron microprobe (**Fig. 7; Supplementary Table 4**). Concentrations broadly split the analyses into two groups, and these groups correlate directly to the chromite content of the grains. High-Cr oxides are enriched in V, Mn, Cu, Zn, and U, and depleted in Ni compared to the low-Cr group. The difference is particularly striking for Zn, with the high-Cr group having concentrations up to 1.4 wt.%, whereas the low-Cr group has a Zn content on the order of tens of ppm. The low-Cr group represents a later generation compared to the high-Cr group, as seen from their textural relationships in thin section. There is a consistent decrease in Zn content, as well as in the other elements associated with decreasing Cr-content in the high-Cr group. There are also region-specific compositional features. For examples, oxides from the Iterlak serpentinites are characteristically rich in Ga, but low in Ti and Mn, and this persists when the oxide composition is divided by its host rock bulk composition.

5.5. Re-Os isotope data

We have measured the Re-Os isotope compositions in three serpentinite samples in order to calculate the time when melt was last extracted from them, assuming that they may represent mantle

residues. Alternatively, in the case of a magmatic origin of the serpentinites the Re-depletions ages may represent their final metamorphic resetting and/or interaction with metasomatic fluids. The Re-Os isotope data are presented in **Supplementary Table 5.** Furthermore, we have recalculated existing Re-Os data from regional subcontinental lithospheric mantle xenoliths (Wittig et al., 2010), by using the same parameters that we use below to make a direct comparison possible.

The Tartoq Group serpentinite samples have γOs ranging from -12.0 to -15.5, using the chondrite values of Shirey and Walker (1998). The model ages (T_{MA}) are ca. 2650, 3650 and 3500 Ma and their corresponding Re-depletion ages (T_{RD}) are ca. 2300, 2800 and 2950 Ma.

6. Discussion

6.1. Alteration and element mobility

The geochemical signatures of the Tartoq Group serpentinites have to be treated with caution to avoid over-interpretation, because the trace element abundances are generally low, with several element concentrations being below their respective detection limits, which makes them susceptible to compositional overprinting. Furthermore, the complex history of these Mesoarchaean rocks, involving metasomatism and metamorphism, will likely have modified their primary compositions, as also documented in other supracrustal belts in SW Greenland (e.g., Polat and Hofmann, 2003; Ordóñez-Calderón et al., 2008; Szilas and Garde, 2013). It is well-established that serpentinisation during seawater interaction results in enrichment in large ion lithophile elements (LILE) and LREE (resulting in positive Eu anomalies), as well as carbonate-hosted trace elements (Pb and Sr) when accompanied by carbonation (Niu, 2004; Paulick et al. 2006; Kodolányi et al., 2012; Marchesi et al., 2013a). We note that Sr is actually lost in these serpentinites, which could either be due to

alteration or because plagioclase phenocrysts retained Sr in the magmas. MgO can show considerable depletion or enrichment depending on the temperature at which the serpentinisation occurs, but commonly MgO-loss is observed during seafloor weathering (Snow and Dick, 1995). Similar element mobility is observed during high-temperature serpentinisation by crustal-derived fluids (Liu et al., 2008; Deschamps et al., 2013; Xie et al., 2013).

SiO_2 is generally not affected by serpentinisation, however, given the large chemical gradient between the serpentinites and the surrounding TTG gneisses, it is not unlikely that mobilisation of SiO_2 into the serpentinites could have occurred to at least some degree. If this was the case, then it would obviously affect our calculations of the normative mineralogy of the protolith for the serpentinites, and subtraction of silica would result in dunitic rather than harzburgitic compositions.

6.2. Bulk-rock major and trace element signatures

In the following we compare the compositions of the Tartoq Group serpentinites with geochemical data for ultramafic rocks from a broad range of geodynamic settings, with the aim of identifying, or at least narrowing down, the possible origins of these serpentinites.

When considering potential protoliths for the Tartoq Group serpentinites their very high MgO contents (34.94-41.95 wt.%) and their generally low trace element abundances rule out a picritic or komatiitic magma origin (**B5-B8**). The tight clustering of MgO concentrations in the serpentinites is a first-order argument against an origin as a fractionation series derived from komatiite/picrite magmas, as discussed below. Given our large and representative sample set of the Tartoq Group, the observed bimodal MgO variation is not consistent with continuous evolution of high-Mg magmas and in particular the elevated FeOt in the serpentinites is not similar to any of these ultramafic magmas.

293 We have compared our serpentinite data with the extensive komatiite data set of Fiorentini et al.
294 (2011) in Figures **B5** and **B6**. Primary komatiite liquids have MgO ranging from 18 to 30 wt.%
295 (Arndt et al., 2008), which is significantly lower than the median value of 39 wt.% for the Tartoq
296 Group serpentinites. Although these serpentinites would fall on the high-MgO cumulate part of the
297 magmatic trend in variation diagrams for komatiites, there are important differences in their FeOt
298 content (**Fig. B5**). It is also clear that only cumulates derived from komatiites can attain these low
299 incompatible element abundances, but that the geochemical compositions of the corresponding
300 Tartoq Group basalts are not consistent with a komatiitic origin (**Fig. B6**). The narrow MgO range
301 of the serpentinites and the relatively low MgO (4.2-16.4 wt.%) of the Tartoq Group basalts is
302 therefore not consistent with derivation of either from continuous fractionation of a komatiite
303 magma.
304 We have also compared the Tartoq Group serpentinites with picrites from the Georoc database
305 (2013), as illustrated in **Figures B7-B8**. As was observed for the komatiite data, the Tartoq Group
306 serpentinites have significantly lower incompatible element abundances and unusually high MgO in
307 comparison with these data. The low incompatible element abundances cannot represent later
308 compositional overprinting of the serpentinites, because the enclosing rocks all have significantly
309 higher concentrations of these elements, and enrichment rather than depletion should thus occur
310 during overprinting. Given that accompanying (more evolved) picritic/komatiitic rocks are not
311 observed anywhere in the Tartoq Group stratigraphy, and that the serpentinites form a tight cluster
312 at around 40 wt.% MgO, and finally that they have FeOt well above the magmatic trends, leads us
313 to exclude an ultramafic magma origin.
314 Even if substantial element mobility had affected the Tartoq Group serpentinites, their
315 systematically low incompatible element compositions and their tight MgO range is not consistent
316 with any known ultramafic magma composition. We can additionally rule out a boninitic origin due

317 to the undepleted trace element patterns and the relatively low SiO_2 of the Tartoq Group basalts.
318 Furthermore, we can rule out that the serpentinites represent cumulates derived from such picritic,
319 komatiitic or boninitic magmas, because none of these rock types are observed in the Tartoq Group,
320 which is instead entirely dominated by tholeiitic basalts (Szilas et al., 2013a).

321 It is further unlikely that the Tartoq Group serpentinites represent tectonised subcontinental
322 lithospheric mantle (SCLM), because their bulk-rock compositions are significantly different from
323 the regional SCLM data reported by Wittig et al. (2010), as shown in **Figure B9**. The serpentinites
324 are not as depleted in major elements as SCLM xenoliths, which have significantly higher MgO and
325 lower FeOt. The Tartoq Group serpentinites have flat trace element patterns, whereas SCLM
326 xenoliths generally have enriched patterns due to metasomatism (e.g., Wittig et al., 2008; Maier et
327 al., 2012). We do note that peridotites exposed in the Ussuit area along the northern margin of the
328 North Atlantic craton, which were described by Kalsbeek and Manatschal (1999), have similar
329 major and trace element compositions compared to the Tartoq Group serpentinites, except for lower
330 FeOt in the former rocks (**Figs. B10-B11**). These authors interpreted the Ussuit rocks as depleted
331 mantle harzburgites that were related to crustal scale tectonic activity of the Archaean basement.
332 Therefore, these rocks could either represent remnants of dismembered ophiolite mantle or parts of
333 the subcontinental lithospheric mantle. The Tartoq Group is located close to the southern margin of
334 the North Atlantic craton, and therefore the serpentinites could in principle have been sheared off
335 from the SCLM during the Ketilidian collisional orogeny at ca. 1800 Ma (Windley, 1991). Such a
336 scenario has been documented in western Norway by Beyer et al. (2004, 2012). However, with the
337 exception of a similar tectonic setting, there is no geochemical evidence to support this, and we find
338 this model difficult to reconcile with the large geochemical differences between the Tartoq Group
339 serpentinites and the regional SCLM xenolith data. More importantly, neither the metamorphic

grades, nor the deformational textures are compatible with those of the Ketilidian orogen in this part of SW Greenland.

The major and trace element compositions of the Tartoq Group serpentinites are also not consistent with these rocks representing hydrated abyssal or forearc mantle residues (e.g., Bodinier and Godard, 2003). When compared to the abyssal peridotite data set of Niu (2004), it is clear that the Tartoq Group serpentinites are too Fe-rich to represent depleted MORB mantle and they also have higher Nb and LREE contents (**Figs. B12-B13**). In particular, they have nearly flat trace element patterns, whereas abyssal mantle rocks are mostly depleted, although there is some overlap (**Figs. B14**). An even larger discrepancy is observed when compared to Oman mantle peridotites (Godard et al., 2000; Hanghøj et al., 2010) and Mariana fore-arc mantle peridotites , which are strongly depleted (Parkinson and Pearce, 1998) (**Figs. B15-B20**). We also note that the normative olivine compositions suggest fosterite-contents ($Mg\#_{olivine}$) from 73 to 84, which is far too low compared to mantle values ($Mg\#_{olivine}$ ~ 90-92). The large proportion of normative orthopyroxene (up to 56%) is also not consistent with a mantle residue origin, which would be expected to be less than 30% in mantle harzburgites.

Although the Tartoq Group serpentinites clearly do not represent serpentinised residual mantle rocks, it should be pointed out that mantle rocks can become modified by reaction with percolating melts (Kelemen et al., 1992) and that this is the case in many ophiolites and lower arc crust sections worldwide (e.g., Takazawa et al., 1992; Bédard et al., 1998; Kelemen et al., 2003; Garrido et al., 2007; Marchesi et al., 2009). Therefore, we can only conclude that a residual mantle origin is not compatible with the Tartoq Group serpentinite data, but the trace element patterns of the Tartoq Group serpentinites could potentially have been modified by trapped or percolating melts in the case of a melt-mantle reaction origin. However, SiO_2 is not significantly elevated despite large amounts of normative orthopyroxene. The Tartoq Group serpentinites does have trace element

abundances in the same range as has been documented for modern melt-modified mantle rocks (Deschamps et al., 2013). However, we cannot distinguish between melt-mantle reaction products and ultramafic cumulates on the basis of the bulk-rock major and trace element data alone. Platinum-group elements may help with discrimination of these two possibilities as explained in the following section.

6.3. Platinum-group element patterns

The previous discussion has allowed us to eliminate several possible origins for the Tartoq Group serpentinites (i.e., picritic/komatiitic/boninitc magmas, mantle residues and tectonised subcontinental mantle), so that only two likely candidates for their protoliths remain: 1) ultramafic cumulates or 2) melt-mantle reaction products. Unfortunately, both of these lithologies share many major and trace element characteristics, as a result of interactions between olivine, orthopyroxene and percolating or trapped melts. It is therefore impossible to differentiate between the two origins based on bulk-rock major and trace element data alone. Ideally, primary mineral compositions would be used, but as we explain in **Section 6.4** below, there is good evidence to suggest that the Tartoq Group serpentinites have been completely overprinted by metamorphic and metasomatic processes and no primary minerals remain.

The platinum-groups elements (PGEs) remain largely immobile during alteration and metamorphism (e.g., Barnes et al., 1985; Crocket, 2000; Wang et al., 2008). Only extensive oxidation during soil and gossan formation, not observed in the Tartoq Group, can lead to significant mobility (Suárez et al., 2010), although Pt and Pd can also be lost during serpentinisation (Lorand, 1989; Alard et al., 2000; Guillot et al., 2000; Marchesi et al., 2013b). The PGEs thus provide a robust indicator of serpentinite protolith, and mantle residues and cumulates can

potentially be distinguished on the basis of their Ir abundances and their general PGE patterns (Hattori and Hart, 1997; Hattori and Shirahase, 1997; Guillot et al., 2000; Hattori et al., 2010). PGEs are highly compatible in the mantle, where they are controlled by monosulfide solid solutions (MSS) and sulfide liquids (Li et al., 1996; Alard et al., 2000; Ballhaus et al., 2006; Luguet et al., 2007; Lorand et al., 2008). As shown in these studies, alloys and MSS determines the abundances of iridium-type PGEs (IPGEs: Os, Ir and Ru), whereas platinum-type PGEs (PPGEs: Pt, Pd, Rd) are highly compatible in Cu-Ni-rich sulfides. In general, mantle peridotites have flat chondrite-normalised PGE patterns at about 0.01 times chondritic values, but can also have minor loss of Pt and Pd, depending on the geological setting in which they formed, their degree of melt depletion and if they were later modified by metasomatism (Rehkämper et al., 1997; Lorand et al., 2008; Hanghøj et al., 2010).

During mantle melting, however, PPGEs behave moderately incompatible, so that the derived melts will have positively fractionated PGE patterns (e.g., Barnes and Picard, 1993). Furthermore, evolution of the magmas during fractional crystallisation will tend to increase Pd/Ir ratios of the melts (Maier and Barnes, 2004), and thus the corresponding cumulates will have low Pd/Ir due to precipitation of compatible IPGE-rich phases. Therefore, mantle melts and their derived cumulates have characteristic positively fractionated PGE patterns due to the strongly compatible nature of IPGEs and the moderately incompatible behaviour of PPGEs (Momme et al., 2002; Woodland et al., 2002; Bézos et al., 2005; Fiorentini et al., 2011; Peucker-Ehrenbrink et al., 2012). Cumulate PGE patterns can additionally become fractionated by accumulation of PGE-rich phases.

The positive Ru anomalies that we observe for the low-Ir group could potentially be explained by accumulation of chromite, which has high partition coefficients for Ru (Capobianco and Drake, 1990; Economou-Eliopoulos and Vacondios, 1995; Ballhaus et al., 2006; Locmelis et al., 2011). We note a strong correlation between the occurrence of magnetite/chromite boxwork/mesh textures (as

412 seen in the Amitsuarsua sliver) and flattish PGE patterns (high-Ir group), in contrast to the presence
413 of magnetite/chromite veining and fractionated PGE patterns (low-Ir group). It would appear that
414 the textures and distribution of chromite is directly responsible for the PGE patterns and in
415 particular the abundances of Os and Ir, which are mainly responsible for the two different patterns
416 (**Fig. 6**). This could in part, be due to differences in IPGE-rich alloys included in chromite.
417 The PGE patterns of the Tartoq Group serpentinites are significantly different from the Oman
418 mantle peridotites of Hanghøj et al. (2010), which are generally flat at about 0.01 times chondritic
419 values (**Fig. B21**). However, there is some resemblance between the PGE patterns from the local
420 SCLM xenoliths of Pyramidefjeld (Wittig et al., 2010) and the high-Ir samples as seen in **Figure**
421 **B22**. Similar PGE patterns are also observed for some of the SCLM xenolith data from South
422 Africa and Finland reported by Maier et al. (2012). Although the PGE patterns of the Tartoq Group
423 serpentinite have some resemblance to those observed for SCLM, we have already ruled out a
424 SCLM origin based on the highly dissimilar major and trace element abundances.
425 Overall, the PGE patterns of the high-Ir group are compatible with a mantle origin for their
426 protoliths (e.g., Hattori and Hart, 1997; Hattori and Shirahase, 1997; Guillot et al., 2000; Hattori et
427 al., 2010). Thus a melt-mantle reaction origin cannot be completely rejected. However, high degree
428 melting (>30%) of mantle can also lead to PGE abundances in the range observed for the high-Ir
429 group, as for example, for komatiite cumulates in the database of Fiorentini et al. (2011), although
430 komatiites do not have as fractioned PGE patterns as the Tartoq Group serpentinites (**Fig. B23**). We
431 consider that the high degrees of mantle melting, that were achieved during the Archaean (Herzberg
432 et al., 2010), would likely result in elevated IPGE abundances in cumulates derived from mantle
433 melts. The high Os-Ir contents of the high-Ir group could imply cumulate precipitation of IPGE-
434 alloys, likely included in chromite. A cumulate origin is thus consistent with PGE concentrations
435 and patterns observed in the Tartoq Group serpentinites. The PGE data for the low-Ir group

conclusively indicates a cumulate origin based on the lower Os and Ir and the positive Ru anomaly. The latter suggests accumulation of either chromite or orthopyroxene in which Ru is compatible (Ballhaus et al., 2006, Luguet et al., 2007).

6.4. Mineral compositions

As mentioned in **Section 1**, petrogenetic studies of serpentinites are made difficult by the obliteration of primary minerals due to hydration and breakdown of mafic minerals, as well as oxides such as spinel. Bernstein et al. (2013) found that Fe^{3+}# can be used as a guide to identify primary spinel compositions in mantle xenoliths by having Fe^{3+}# < 10. A similar value of Fe^{3+}# < 12 was used by Hattori and Guillot (2007) for identification of primary spinel in Himalayan serpentinised mantle chromites. However, as seen by the elevated Fe^{3+}# of the Tartoq Group chromites (>55), metasomatic disturbance and oxidation has affected these minerals significantly (**Fig. B4**). This is also indicated by the very low Mg# (<2) in combination with high Cr# (>74) as seen in **Figure B3**, which are unlike primary magmatic or mantle-related chromites (e.g., Arai et al., 1992; Parkinson and Pearce, 1998; Barnes and Roedder, 2001; Matsukage and Kubo, 2003). We interpret grains with low chromite content as late-stage growth and replacement, although none of these grains represent primary compositions, as metamorphism generally shifts magmatic compositions to high Cr# and Mg# (Evans and Frost, 1974; Barnes and Roedder, 2001). Thus, we consider that metasomatic disturbance has completely reset the major element compositions of spinel in the Tartoq Group serpentinites, which is also supported by the very low Al and Mg content measured with LA-ICP-MS (**Section 6.5**).

Similar resetting of chromites is reported by Bazylev et al. (2013) in lower crustal ultramafic rocks and by O'Hanley (1996) and Säntti et al. (2006) for serpentinites metamorphosed at

amphibolite facies conditions. Even more relevant for our serpentinites is the study of the Isua supercrustal rocks by Rollinson (2007), who found similar Mg# and Cr# for spinels in serpentinites associated with those rocks. The geological setting and metamorphic conditions of these two different supracrustal associations are indeed very similar (Kisters et al., 2012; Rollinson, 2002). These results therefore suggest that primary magmatic chromite is unlikely to survive serpentinisation followed by amphibolite facies metamorphism.

6.5. In situ chromite trace element compositions

As stated above, the major element compositions of the oxides have experienced complete resetting. The question is then whether or not any of the trace elements in these chromites have preserved their primary compositions. **Figure 7** shows the Tartoq Group chromites normalised to MORB chromites. These chromites have likely experienced very reducing conditions due to release of H_2 during serpentinisation. This would have had a strong effect on the compatibility of the transition metals (Ti, V, Co, Zn and Cr), which indeed show large total variability. Zinc is positively correlated with Cr, and so are Co and V to some degree, whereas Fe and Cr are negatively correlated. These relations among the transition metals suggest consistent partitioning behaviour. But because there are no systematic variations between cores and rims, and the fact that the major element compositions of the chromite are certainly disturbed by metasomatism, it appears unlikely that any of the trace element variation records primary compositions. The specific trace element abundances are likely a function of the local composition of the metamorphic fluids and the compositions of the mineral phases that were in immediate contact with the chromites. Thus, for lack of preservation, we are unable to use the major or trace element composition of Tartoq oxides to determine the origin of their ultramafic host rocks. In particular the very low Al and Mg contents

484 of the Tartoq Group chromites is unlike those found in MORB or boninites, which suggests that
485 these are not primary magmatic compositions (**Fig. 7**).
486
487 6.6. Isotope constraints
488
489 The observation that the calculated Re-depletion ages (T_{RD}) are younger that the minimum age of
490 2986 Ma for the Tartoq Group (Szilas et al., 2013a), strongly suggest that the Re-Os isotope
491 compositions of the serpentinites were overprinted after extrusion of the Tartoq Group volcanic
492 sequence. Metamorphism and metasomatism have indeed recently been shown to have the ability to
493 disturb the Re-Os isotope system (Gonzáles-Jiménez et al., 2012; Lorand et al., 2012). Bulk-rock
494 Re-depletion ages thus only represent minimum ages. However, the true magmatic age may be
495 preserved within single minerals (Bragagni et al., 2013; González-Jiménez et al., 2013). Therefore it
496 is possible that our bulk-rock Re-depletion ages record the final terrane assembly/metamorphism if
497 Re was introduced by early melt-rock reactions and was lost during later metamorphism.
498 Alternatively, metasomatic fluids could have brought in Os with a different isotope composition,
499 which overprinted the primary magmatic depletion ages.
500 When we compare our new Re-Os isotope data with those published for regional SCLM
501 xenoliths it is apparent that the Tartoq Group serpentinites preserve some of the oldest Re-depletion
502 ages in SW Greenland (**Supplementary Table 5**). Although the geochemical compositions of the
503 serpentinites are very different from those of the SCLM xenoliths, it is possible that they originally
504 formed in a similar geological setting and that their differences simply reflect dissimilar evolution
505 in terms of initial melt depletion, metamorphism and metasomatic history.
506 Szilas et al. (2013a) reported εNd_{3190Ma} of +3.0 ±0.4 and εHf_{3190Ma} of +2.1 ±0.5 for one
507 serpentinite sample (510766). This result plots right on the depleted mantle (DM) evolution of the

Sm-Nd system, but about 4 ε-units below the Lu-Hf evolution of the DM (Griffin et al., 2000). The large discrepancy between these two isotope systems is best interpreted as resulting from disturbance of the Lu-Hf systematics due to lack of an appropriate mineral host for Hf in the serpentinites. This is consistent with their extremely low Hf abundances, so they would be prone to crustal contamination and overprinting of their Hf-isotope compositions. However, the fact that εNd_{3190Ma} does indeed plot on the DM evolution line, is not robust evidence for derivation from this source, but could equally well reflect interaction with percolating melts from this source. The latter interpretation would indeed be consistent with the relatively flat melt-like trace element patterns that are observed for the serpentinites, as discussed in **Section 6.2**. On the other hand these observations are also consistent with a cumulate origin, if they were in equilibrium with the Tartoq Group volcanic rocks. In conclusion, the possibility of younger metasomatism and melt percolation in these rocks, limits the usefulness of the Re-Os, Sm-Nd and Lu-Hf isotope systems with regards to the discrimination between a cumulate and a mantle origin of the Tartoq Group serpentinites.

6.7. Petrogenetic implications

There is mounting consensus that the Mesoarchaean supracrustal belts of SW Greenland represent formation in subduction zone settings (e.g., Klausen et al., 2011; Ordóñez-Calderón et al., 2011; Polat et al., 2011; Szilas et al., 2012a, 2012b, 2013b, in press; Furnes et al., 2013). The overall island arc-like geochemical features of the Tartoq Group mafic tholeiitic rocks (Szilas et al., 2013a), are consistent with such an origin, and this is further supported by the Tartoq Group structures (Kisters et al., 2012). In the following, we therefore explicitly compare the Tartoq Group lithologies to published arc sequences.

The geochemical data for the Tartoq Group displays a good overlap with data from the Mesozoic Kohistan Island Arc (**Figs. B24-B25)**. Interestingly, the ultramafic lithologies of the Kohistan sequence show similar ranges in both major and trace elements, as the Tartoq Group serpentinites. In particular, we find that the similarities that are observed in the ranges of MgO, FeOt, Al_2O_3, Ni and Cr between the Tartoq Group serpentinites and the ultramafic section of the Kohistan Arc Complex provides the best fit of all rocks with which we have compared our data. This suggests that similar magmatic processes could explain these rock assemblages (**Fig. 8**).

Unfortunately, the petrogenetic interpretation of the Kohistan ultramafic rocks is ambiguous and explanations include origins as ultramafic cumulates, as well as melt-modified mantle rocks (Jagoutz et al., 2006; Garrido et al., 2007; Jagoutz et al., 2011; Jagoutz and Schmidt, 2012). No detailed discussion of platinum-group element data is available for the Kohistan Island Arc, and the data are limited to two abstracts (Hattori and Hart, 1997; Hattori and Shirahase, 1997). The fact that controversy still surrounds the origin of the ultramafic rocks of the relatively fresh and well-studied Kohistan Arc Complex, shows that this geological problem is difficult to solve. In fact, it has only recently been possible to discriminate between peridotitic melt-mantle reaction products and cumulates in the extremely well-preserved peridotites of the Massif du Sud Ophiolite in New Caledonia (Pirard et al., 2013) and the Oman Ophiolite (Abily and Ceuleneer, 2013). Detailed PGE data, which could have suggested a clear discriminant applicable to the overprinted Tartoq Group serpentinites, are lacking for both of these occurrences.

Geochemical and lithological similarities are also seen between the Talkeetna arc section and the Tartoq Group (**Fig. B26-B27**). The slightly higher SiO_2 in the Tartoq Group serpentinites relative to the dunites of the Kohistan and Talkeetna Arc Complexes could be explained if the protoliths of the Tartoq Group serpentinites were not dunites, but harzburgites as indeed suggested by their normative mineralogy (**Fig. B2**). However, SiO_2 and MgO are notoriously mobile in

555 metamorphosed Archaean supracrustal rocks (e.g., Polat and Hofmann, 2003; Szilas and Garde,
556 2013), and the small discrepancies between fresh ultramafic rocks and the Tartoq Group
557 serpentinites are inconsequential considering the tectonic and metamorphic history of the latter. As
558 is the case for the Kohistan section, it is difficult to pinpoint where the actual contact between
559 ultramafic cumulates and the mantle occurs in the Talkeetna arc, which is made additionally
560 difficult because it is unknown how much of the cumulate section has delaminated from the base of
561 the arc (DeBari and Coleman, 1989; Greene et al., 2006; Hacker et al., 2008; DeBari and Greene,
562 2011). Thus, it seems that at the present there is no consensus regarding the exact petrological
563 origin of the lowermost ultramafic portion of island arc complexes, i.e. mantle vs. magmatic
564 cumulate.

565 One key-feature of the Tartoq Group serpentinites, in addition to the PGE argument presented
566 above, that makes us propose a cumulate origin, rather than a melt-modified mantle origin, is their
567 high FeOt (9.5-17.3 wt.%) leading to bulk Mg# of 80-88. If we assume that these Mg#'s reflect
568 those of the primary rock and that serpentinisation and metamorphism did not significantly affect
569 MgO and FeOt, then the Mg# is much too low to be of mantle origin. Although minor Fe-mobility
570 is observed in the Tartoq Group serpentinites, it appears restricted to segregation of magnetite,
571 rather than significant Fe-metasomatism. This is supported by the global serpentinite database of
572 Deschamps et al. (2013), which is dominated by mantle-derived rocks in which Fe-rich
573 serpentinites are relatively rare. In contrast cumulate peridotites are commonly Fe-rich (e.g.,
574 Nielsen, 1981; Johnson et al., 2004; Liu et al., 2008; Thakurta et al., 2008). Our preferred
575 interpretation of the Tartoq Group serpentinites is thus that they represent harzburgitic cumulates
576 derived from magmas that formed by variable degrees of partial melting of an arc-related mantle
577 source. Large degree melts resulted in the high-Ir group, whereas lower degrees of melting formed

578 the low-Ir group. However, it is also possible that these two groups simply represent early and late
579 cumulates, respectively.

580 Given that a harzburgitic normative composition dominates the protoliths of the Tartoq Group
581 serpentinites, we can rule out a cumulate origin derived from anhydrous magmas, because these
582 would crystallise plagioclase after olivine, whereas H_2O depresses the crystallisation of plagioclase
583 and additionally pushes resulting cumulates to harzburgitic compositions (Müntener et al., 2001;
584 Feig et al., 2006; Müntener and Ulmer, 2006). Furthermore, the apparent absence of clinopyroxene,
585 evidenced by low CaO and Al_2O_3 content, and hence the potential crystallisation of orthopyroxene
586 indicates that the mantle source was either depleted harzburgite or that the primary magma was
587 relatively silicious (e.g., Tatsumi, 1981; Umino and Kushiro, 1989; Wood and Turner, 2003). One
588 alternative possibility, which cannot be ruled out from the present data, is that the normative
589 orthopyroxene could be a result of reaction between dunite cumulates and trapped inter-cumulus
590 melt (see below), which would also explain the relatively elevated incompatible trace element
591 abundances of the Tartoq Group serpentinites.

592 All of the above considerations are consistent with the arc-affinity of the Tartoq Group volcanic
593 sequence and thus an origin of the protoliths of the serpentinites as harzburgitic cumulates. Finally,
594 our trace element modelling of the evolution of the tholeiitic basalt during fractional crystallisation
595 of olivine (69%), orthopyroxene (30%) and chromite (1%), fit reasonably well with the observed
596 ranges for the more compatible trace elements (e.g., Ni, Cr, Co, Sc) and suggests about 30% melt
597 crystallisation from least to most evolved sample (**Fig. B28**). The incompatible trace element ratios
598 are largely unaffected by crystallisation of this ultramafic cumulate as would be expected, and the
599 residual enrichment in the magmas also fit well with the observed evolution of the Tartoq Group
600 mafic sequence (**Fig. B29**). The major element variation is also compatible with fractional
601 crystallisation of olivine and orthopyroxene from the mafic sequence in the Tartoq Group (**Fig.**

602 **B30**). However, it should be noted that this model would not be significantly different if only
603 olivine and chromite crystallised.

604 Finally, we have tested the cumulate model by calculating the liquid line of descent of our data
605 set using the Melts software (Ghiorso and Sack, 1995; Asimow and Ghiorso, 1998). We used one of
606 the least evolved samples (510687) that we considered to represent a primitive liquid, as the starting
607 composition. Oxygen fugacity was buffered at QFM, pressure was kept constant at 2 Kb, initial
608 H_2O was arbitrarily assumed to be 0.5 wt.% and we used a fractional model from 1310°C to 1150°C
609 at 10° intervals. **Figure 9** shows that the model is able to reproduce much of the major element
610 variation, although the match is obviously not perfect. The corresponding bulk cumulate is even
611 more depleted than the Tartoq Group serpentinites and variable degrees of trapped inter-cumulus
612 liquid would be able to explain the major element compositions, as well as the elevated
613 incompatible trace element abundances of the serpentinite protolith. A rough mass balance suggests
614 that these cumulate rocks consisted of up to 25% trapped liquids. Most importantly, the modelled
615 cumulates would have up to 13 wt.% FeOt, which support a primary cumulate origin of the
616 serpentinites. SiO_2 is also elevated in the serpentinites relative to the calculated cumulate. This
617 could either be due to reaction with trapped inter-cumulus melts or silica metasomatism during
618 metamorphism/alteration. Both of these scenarios would explain the normative orthopyroxene in
619 these rocks without a need for fractional crystallisation of this particular mineral. The model does
620 not take into account that sulfide liquids may also have precipitated with these cumulates and this
621 may explain why Ni is too low in our model (not shown), or alternatively the partition coefficient
622 was incorrect for the given conditions. Likewise, chromitite formation in other parts of the cumulate
623 pile or within the delaminated mantle section could potentially explain the observed lower Cr
624 contents in the serpentinites. In summary, we find that an olivine-dominated cumulate, which

reacted with trapped inter-cumulus melts, would indeed be able to produce the observed bulk compositions of the Tartoq Group serpentinites.

Regardless of whether we can conclusively distinguish between a melt-modified mantle or a cumulate origin for the Tartoq Group serpentinite protoliths, a likely geological setting for these rocks would be at the ultramafic crust-mantle interface, i.e., the petrological Moho. This is entirely compatible with the previous interpretation of the Tartoq Group as remnants of arc-related oceanic fore-arc or back-arc crust (Szilas et al., 2013a). Therefore, the Tartoq Group essentially represents an arc-related ophiolite section (cf., Dilek and Polat, 2008; Dilek and Furnes, 2011; Furnes et al., 2013). Moreover, Kisters et al. (2012) proposed that the Tartoq Group accreted in a convergent margin based on the structural characteristics of these rocks. This would be consistent with the observation that serpentinisation in fore-arcs has an important role in the development of shear zones, thrusting and obduction of arc-related oceanic crust (e.g., Bostock et al., 2002; Lee et al., 2008). The serpentinites were thrust from the base of the Tartoq Group (regardless of their origin) and are now found along structural features, as observed in the Amitsuarsua, Bikuben and Iterlak slivers (**Figs. 1 and 2**).

Overall, the broad suite of geological and geochemical evidence from the Tartoq Group points to its formation in an arc-related environment. This has important implications for understanding Archaean geodynamics, because it indicates that subduction-zone processes were operating in the Mesoarchaean. This conclusion adds to a growing body of evidence from a diverse range of studies, which all suggest that modern-style tectonic processes began before 3 Ga (e.g., Shirey and Richardson, 2011; Dhuime et al., 2012; Næraa et al., 2012; Hynes, 2013; Szilas et al., 2013b; Gerya, 2014).

7. Conclusions

- The Tartoq Group serpentinites have bulk-rock geochemical compositions, which are significantly different from ultramafic magmas (picrites/boninites/komatiites), as well as from mantle residues (both abyssal and arc-related) or subcontinental lithospheric mantle (SCLM) xenoliths. In particular, the bimodal rather than a continuous variation, does not support an ultramafic magma origin.
- Based on the bulk-rock geochemical data and their normative harzburgitic composition, we find that the Tartoq Group serpentinites share many similarities with peridotitic cumulates or melt-modified mantle rocks.
- The chondrite-normalised platinum-group element (PGE) patterns are compatible with both cumulate and melt-modified mantle origins for the high-Ir group Tartoq Group serpentinites, whereas the low-Ir group is best interpreted as of magmatic cumulate origin.
- Although it proves challenging to conclusively distinguish between a cumulate and a melt-modified mantle origin for these serpentinites, we prefer the former model owing to the fractionated PGE patterns and the elevated FeOt content (9.5-17.3 wt.%), which is much higher than what is found in mantle rocks, but within the range of peridotitic cumulates. The Cr and Ni ranges are also more compatible with a cumulate than a mantle origin.
- A cumulate origin is also supported by modelling using the MELTS software (Ghiorso and Sack, 1995; Asimow and Ghiorso, 1998). In particular, the model results in FeOt up to 13 wt.%, which is unique to ultramafic cumulates relative to magmas and mantle residues.
- Laser ablation and electron microprobe analysis of magnetite and chromite in the serpentinites indicates significant metasomatic overprint of these minerals. Thus, they do not preserve any primary petrogenetic information.

- Re-Os isotope data suggests that the serpentinites have experienced post-magmatic disturbance, although not to the same degree as the regional SCLM (Wittig et al., 2010) and thus record the oldest Re-depletion events (T_{RD}) in this region with ages up to ca. 2950 Ma.
- Overall, we interpret the bulk-rock geochemical data for the Tartoq Group serpentinites as being consistent with an origin as lower crustal ultramafic cumulates, which formed by fractional crystallisation of olivine and chromite, only joined by plagioclase at late stages. The negligible normative plagioclase and clinopyroxene in these cumulates, suggest hydrous melting conditions of the mantle source, possibly in combination with contamination with silica to displace the melt evolution to crystallise early orthopyroxene instead of clinopyroxene. Alternatively, the normative orthopyroxene could reflect reaction between dunite cumulates and trapped inter-cumulus melt, which is indeed suggested by the elevated incompatible trace element abundances in the serpentinites.

Acknowledgements

We thank the Geological Survey of Denmark and Greenland (GEUS) and the Bureau of Minerals and Petroleum (BMP) for funding the fieldwork and for permission to publish these results. K. Szilas acknowledges support from The Danish Council for Independent Research - Natural Sciences (FNU) via grant no. 12-125873. V.J. van Hinsberg acknowledges financial support from the Natural Sciences and Engineering Research Council of Canada (NSERC). This paper is a contribution to IGCP Project 599. We acknowledge Marco Scambelluri for the editorial handling of the manuscript. We are grateful for critical comments provided by Claudio Marchesi, Hugh Rollinson and one anonymous reviewer, which significantly improved this paper.

References

Abily, B., Ceuleneer, G., 2013. The dunitic mantle-crust transition zone in the Oman ophiolite: Residue of melt-rock interaction, cumulates from high-MgO melts, or both? Geology 41, 67-70.

Alard, O., Griffin, W.L., Lorand, J.P., Jackson, S.E., O'Reilly, S.Y., 2000. Non-chondritic distribution of highly siderophile elements in mantle sulfides. Nature 407, 891-894.

Appel, P.W.U., 1984. An iron-formation in the Precambrian Tartoq Group, South-West Greenland. Rapport Grønlands Geologiske Undersøgelse 120, 74-78.

Appel, P.W.U., Secher, K., 1984. On gold mineralization in the Precambrian Tartoq Group, SW Greenland. Journal of the Geological Society, London 141, 273-278.

Arai, S., 1992. Chemistry of chromian spinel in volcanic rocks as a potential guide to magma chemistry. Mineralogical Magazine 56, 173-184.

Arndt, N., Lesher, M.C., Barnes, S.J., 2008. Komatiite. Cambridge University Press, 467 pp.

Asimow, P.D., Ghiorso, M.S., 1998. Algorithmic modifications extending MELTS to calculate subsolidus phase relations. American Mineralogist 83, 1127-1132.

Ballhaus, C., Bockrath, C., Wohlgemuth-Ueberwasser, C., Laurenz, V., Berndt, J., 2006. Fractionation of noble metals by physical processes. Contribution to Mineralogy and Petrology 152, 667-684.

720 Barnes, S.J., Roedder, P.L. 2001. The range of spinel compositions in terrestrial mafic and
721 ultramafic rocks. Journal of Petrology 42, 2279-2302.
722
723 Barnes, S.-J., Naldrett, A.J., Gorton, M.P., 1985. The origin of fractionation of platinum-group
724 elements in terrestrial magmas. Chemical Geology 53, 303-323.
725
726 Barnes, S.-J., Picard, C.P., 1993. The behavious of platinum-group elements during partial melting,
727 crystal fractionation, and sulphide segregation: An example from the Cape Smith Fold Belt,
728 northern Quebec. Geochimica et Cosmochimica Acta 57, 79-87.
729
730 Bazylev, B.A., Ledneva, G.V., Kononkova, N.N., Ishiwatari, A., 2013. High-pressure ultramafics in
731 the lower crustal rocks of Pekul'ney Complex, Central Chukchi Peninsula. 1. Petrography and
732 mineralogy. Petrology 21, 221-248.
733
734 Bédard, J.H., Lauziere, K., Tremblay, A., Sangster, A., 1998. Evidence for forearc seafloor-
735 spreading from Betts cove ophiolite, Newfoundlander: Oceanic crust of boninitic affinity.
736 Tectonophysics 284, 233-245.
737
738 Bernstein, S., Szilas, K., Kelemen, P.B., 2013. Highly depleted cratonic mantle in West Greenland
739 extending into diamond stability field in the Proterozoic. Lithos 168-169, 160-172.
740
741 Berthelsen, A., Henriksen, N., 1975. Geological map of Greenland, 1:100,000 Ivittuut 61 V.1 Syd
742 (with description), Geological Survey of Greenland, Copenhagen, 169 pp.
743

744 Beyer, E.E., Brueckner, H.K., Griffin, W.L., O'Reilly, S.Y.O., Graham, S., 2004. Archean mantle
745 fragments in Proterozoic crust, Western Gneiss Region, Norway. Geology 32, 609-612.
746
747 Beyer, E.E., Brueckner, H.K., Griffin, W.L., O'Reilly, S.Y.O., 2012. Laurentian provenance of
748 Archean mantle fragments in the Proterozoic Baltic crust of Norwegian Caledonides. Journal of
749 Petrology 53, 1357-1383.
750
751 Bézos, A., Lorand, J.-P., Humler, E., Gros, M., 2005. Platinum-group element systematics in mid-
752 ocean ridge basaltic glasses from the Oacific, Atlantic and Indian Oceans. Geochimica et
753 Cosmochimica Acta 69, 2613-2627.
754
755 Bodinier, J.L., Godard, M., 2003. Orogenic, ophiolitic, and abyssal peridotites. Treatise on
756 Geochemistry, vol. 2, 103-170.
757
758 Bostock, M.G., Hyndman, R.D., Rondenay, S., Peacock, S.M., 2002. An inverted continental Moho
759 and serpentinisation of the forearc mantle. Nature 417, 536-538.
760
761 Bragagni, A., Luguet, A., Pearson, D.G., Fonseca, R.O.C., Kjarsgaard, B.A., 2013. Mineralogical
762 Magazine, 77, 760.
763
764 Capobianco, C.J., Drake, M.J., 1990. Partitioning of ruthenium, rhodium, and palladium between
765 spinel and silicate melt and implications for platinum group element fractionation trends.
766 Geochimica et Cosmochimica Acta 54, 869-874.
767

768 Crocket, J.H., 2000. PGE in fresh basalt, hydrothermal alteration products, and volcanic
769 incrustations of Kilauea volcano, Hawaii. Geochimica et Cosmochimica Acta 64, 1791-1807.
770
771 DeBari, S.M., Coleman, R.G., 1989. Examination of the deep levels of an island arc: evidence from
772 the Tosina ultramafic-mafic assemblage, Tosina, Alaska. Journal of Geophysical Research 94,
773 4373-4391.
774
775 DeBari, S.M., Greene, A.R., 2011. Vertical stratification of composition, density, and inferred
776 magmatic processes in exposed arc crustal sections. In: Brown, D. and Ryan, P.D. (Eds.). Arc-
777 continent collision. Springer Berlin Heidelberg, pp. 121-144.
778
779 Deschamps, F., Godard, M., Guillot, S., Hattori, K., 2013. Geochemistry of subduction zone
780 serpentinites: A review. Lithos 178, 96-127.
781
782 Dilek, Y., 2003. Ophiolite concept and its evolution. In: Dilek, Y.,Newcomb, S., (Eds.). Ophiolite
783 concept and the evolution of geological thought. Geological Society of America, Special Paper 373,
784 1-16.
785
786 Dilek, Y., Polat, A., 2008. Suprasubduction zone ophiolites and Archean tectonics. Geology 36,
787 431-432.
788
789 Dilek, Y., Furnes, H., 2011. Ophiolite genesis and global tectonics: geochemical and tectonic
790 fingerprinting of ancient oceanic lithosphere. Geological Society of America Bulletin 123, 387-411.
791

792 Dhuime, B., Hawkesworth, C.J., Cawood, P.A., Storey, C.D., 2012. A change in the geodynamics
793 of continental growth 3 billion years ago. Science 335, 1334-1336.
794
795 Economou-Eliopoulos, M., Vacondios, I., 1995. Geochemistry of chomitites and host rocks from
796 the Pindos ophiolite complex, northwestern Greece. Chemical Geology 122, 99-108.
797
798 Evans, B.W., Frost, B.R., 1974. Chrome-spinel in progressive metamorphism – a preliminary
799 analysis. Geochimica et Cosmochimica Acta 39, 959-972.
800
801 Evans, D.M., King, A.R., 1993, Sediment and shear-hosted gold mineralization of the Tartoq Group
802 supracrustals, southwest Greenland. Precambrian Research 62, 61-82.
803
804 Feig, S.T., Koepke, J., Snow, J.E., 2006. Effect of water on tholeiitic basalt phase equilibria: an
805 experimental study under oxidizing conditions. Contributions to Mineralogy and Petrology 152,
806 611-638.
807
808 Fiorentini, M.L., Barnes, S.J., Maier, W.D., Burnham, O.M., Heggie, G., 2011. Global variability in
809 the platinum-group element contents of komatiites. Journal of Petrology 52, 83-112.
810
811 Fisher-Gödde, M., Becker, H., Wombacher, F., 2010. Rhodium, gold and other highly siderophile
812 element abundances in chondritic meteorites. Geochimica et Cosmochimica Acta 74, 356-379.
813
814 Furnes, H., Dilek, Y., de Wit, M., 2013. Precambrian greenstone sequences represent different
815 ophiolite types. Gondwana Research (in press).

816

817 Garrido, C.J., Bodinier, J.-L., Dhuime, B., Bosch, D., Chanefo, I., Bruguier, O., Hussain, S.S.,
818 Dawood, H., Burg, J.-P., 2007. Origin of the island arc Moho transition zone via melt-rock reaction
819 and its implication for intracrustal differentiation of island arcs: Evidence from the Jijal complex
820 (Kohistan complex, northern Pakistan). Geology 35, 683-686.

821

822 Georoc database, http://www.georoc.mpch-mainz.gwdg. de/ (accessed June 2013).

823

824 Gerya, T., 2014. Precambrian geodynamics: Concepts and models. Gondwana Research 25, 442-
825 463.

826

827 Ghiorso, M.S., Sack, R.O., 1995. Chemical mass transfer in magmatic processes IV. A revised and
828 internally consistent thermodynamic model for the interpolation and extrapolation of liquid-solid
829 equilibria in magmatic systems at elevated temperatures and pressures. Contributions to Mineralogy
830 and Petrology 119, 197-212.

831

832 Godard, M., Jousselin, D., Bodinier, J. L., 2000. Relationships between geochemistry and structure
833 beneath a palaeo-spreading centre: a study of the mantle section in the Oman ophiolite. Earth and
834 Planetary Science Letters 180, 133-148.

835

836 Gonzáles-Jiménez, J.M., Griffin, W.L., Gervilla, Kerestedjian, T.N., O'Reilly, S.Y., Proenza, J.A.,
837 Pearson, N.J., Sergeeva, I., 2012. Metamorphism disturbs the Re-Os signatures of platinum-group
838 minerals in ophiolite chromitites. Geology 40, 659-662.

839

González-Jiménez, J.M., Griffin, W.L., Gervilla, F., Proenza, J.A., O'Reilly, S.Y., Pearson, N.J., 2013. Chromitites in ophiolites: How, where, when, why? Part I. A review and new ideas on the origin and significance of platinum-group minerals. Lithos (in press).

Greene, A.R., DeBari, S.M., Kelemen, P.B., Blusztajn, J., Clift, P.D., 2006. A detailed geochemical study of island arc crust: the Talkeetna arc section, South-Central Alaska. Journal of Petrology 47, 1051-1093.

Griffin, W.L., Pearson, N.J., Belousova, E., Jackson, S.E., Van Achterbergh, E., O'Reilly, S.Y., Shee, S.R., 2000. The Hf isotope composition of cratonic mantle: LAM-MC-ICPMS analysis of zircon megacrysts in kimberlites. Geochimica et Cosmochimica Acta 64, 133-147.

Guillot, S., Hattori, K.H., De Sigoyer, J., 2000. Mantle wedge serpentinisation and exhumation of eclogites: insights from eastern Ladakh, northwest Himalaya. Geology 28, 199-202.

Hacker, B.R., Mehl, L., Kelemen, P.B., Rioux, M., Behn, M.D., Luffi, P., Reconstruction of the Talkeetna intraoceanic arc of Alaska through thermobarometry. Journal of Geophysical Research 113, B03204.

Hanghøj, K., Kelemen, P.B., Hassler, D., Godard, M., 2010. Composition and genesis of depleted mantle peridotites from the Wadi Tayin Massif, Oman Ophiolite; major and trace element geochemistry, and Os isotope and PGE systematics. Journal of Petrology 51, 201-227.

Hattori, K., Hart, S.R., 1997. PGE and Os isotopic signatures for ultramafic rocks from the base of the Talkeetna island arc, Alaska. EOS 78, 339.

Hattori, K., Shirahase, T., 1997. Platinum group elements and osmium isotope signatures of the Kohistan island arc sequence, Himalaya-Karakaram area. EOS 78, 829.

Hattori, K.H., Guillot, S., 2007. Geochemical character of serpentinites associated with high- to ultrahigh-pressure metamorphic rocks in the Alps, Cuba, and the Himalayas: Recycling of elements in subduction zones. Geochemistry, Geophysics, Geosystems 8, Q09010.

Hattori, K., Wallis, S., Enami, M., Mizukami, T., 2010. Subduction of mantle wedge peridotites: evidence from the Hihashi-akaishi ultramafic body in the Sanbagawa metamorphic belt. Island arc 19, 192-207.

Herzberg, C., Condie, K., Korenaga, J., 2010. Thermal history of the Earth and its petrological expression. Earth and Planetary Science Letters 292, 79-88.

Higgins, A.K., Bondesen, E., 1966. Supracrustals of pre-Ketilidian age (the Tartoq Group) and their relationships with Ketilidian supracrustals in the Ivigtut region, South-West Greenland. Rapport Grønlands Geologiske Undersøgelse 8, 21 pp.

Higgins, A.K., 1968. The Tartoq Group on Nuna Qaqertoq and in the Iterdlak area, South-West Greenland. Rapport Grønlands Geologiske Undersøgelse 17, 17 pp.

887 Higgins, A.K., 1990. Descriptive text to 1:100000 sheets Neria 61 V.1 N and Midternæs 61 V.2 N.
888 Geological Survey of Greenland, 23 pp.
889
890 Hynes, A.A., 2013. How Feasible Was Subduction in the Archean? Canadian Journal of Earth
891 Sciences (in press).
892
893 Jagoutz, O., Müntener, O., Burg, J.-P., Ulmer, P., Jagoutz, E., 2006. Lower continental crust
894 formation through focused flow in km-scale melt conduits: the zoned ultramafic bodies of the
895 Chilas Complex in the Kohistan island arc (NW Pakistan). Earth and Planetary Science Letters 242,
896 320-342.
897
898 Jagoutz, O., Schmidt, M.W., 2012. The formation and bulk composition of modern juvenile
899 continental crust. Chemical Geology 298-299, 79-96.
900
901 Janosek, V., Farrow, C.M., Erban, V., 2006. Interpretation of whole-rock geochemical data in
902 igneous geochemistry: introducing Geochemical Data Tool (GCDkit). Journal of Petrology 47,
903 1255-1259.
904
905 Johnson, K.E., Brady, J.B., MacFarlane, W.A., Thomas, R.B., Poulsen, C.J., Sincock, M. J., 2004.
906 Precambrian meta-ultramafic rocks from the Tobacco Root Mountains, Montana. Geological
907 Society of America Special Papers 377, 71-88.
908

909 Kalsbeek, F., Manatschal, G., 1999. Geochemistry and tectonic significance of peridotitic and
910 metakomatiitic rocks from the Ussuit area, Nagssugtoqidian orogen, West Greenland. Precambrian
911 Research 94, 101-120.
912
913 Kelemen, P.B., Dick, H.J.B., Quick, J.E., 1992. Formation of harzburgite by pervasive melt/rock
914 reaction in the upper mantle. Nature 358, 635-641.
915
916 Kelemen, P.B., Hart S.R. Bernstein, S., 1998. Silica enrichment in the continental upper mantle via
917 melt/rock reaction, Earth and Planetary Science Letters 164, 387-406.
918
919 Kelemen, P.B., Hanghøj, K., Greene, A., 2003. One view of the geochemistry of subduction-related
920 magmatic arcs, with an emphasis on primitive andesite and lower crust. In: Rudnick R.L. (Ed.), The
921 Crust, Vol. 3, Treatise on Geochemistry. Holland, H.D., Turekian, K.K., (Eds.). Oxford, UK,
922 Elsevier-Pergamon, 593-659.
923
924 King, A.R., 1985. Greenex A/S Sermiligarssuk exploration concession. Report on geological field
925 work carried out in the Sermiligarssuk Fjord area, South-west Greenland, July-August 1984.
926 Greenex A/S, 142 pp.
927
928 Kisters, A.F.M., Szilas, K., Van Hinsberg, V.J., 2011. Structural geology and emplacement of the
929 Tartoq Group, SW Greenland. In: Kolb, J. (Ed.), Controls of Hydrothermal Quartz Vein
930 mineralisation and Wall-rock Alteration in the Paamiut and Tartoq Areas, South-West Greenland.
931 Danmarks og Grønlands Geologiske Undersøgelse Rapport 2011/114, pp. 116-147.
932

933 Kisters, A.F., Van Hinsberg, V.J., Szilas, K., 2012. Geology of an Archaean accretionary complex–
934 The structural record of burial and return flow in the Tartoq Group of South West Greenland.
935 Precambrian Research 220-221, 107-122.
936
937 Klausen, M.B., Kokfelt, T.F., Keulen, N., Berger, A., Schumacher, J.C., 2011. Geochemistry of
938 Archaean serpentinites, tholeiitic amphibolites and calc-alkaline schists across the Nigerlikasik
939 section in the Kvanefjord Terrane, South-West Greenland, ~62°S. Grønlands Geologiske
940 Undersøgelse Rapport 2011/11.
941
942 Kodolányi, J., Pettke, T., Spandler, C., Kamber, B.S., Gméling, K., 2012. Geochemistry of ocean
943 floor and fore-arc serpentinites: constraints on the ultramafic input to subduction zones. Journal of
944 petrology 53, 235-270.
945
946 Lee, C.-T.A., Luffi, P., Höink, T., Li, Z.-X.A., Lenardic, A., 2008. The role of serpentine in
947 preferential craton formation in the late Archean by lithosphere underthrusting. Earth and Planetary
948 Science Letters 269, 96-104.
949
950 Li, C., Barnes, S.-J., Makovicky, E., Rose-Hansen, J., Makovicky, M., 1996. Partintioning of
951 nickel, copper, iridium, rhenium, platinum, and palladium between monosulfide solid solution and
952 sulfide liquid: effect of composition and temperature. Geochimica et Cosmochimica Acta 60, 1231-
953 1238.
954

955 Liu, Y., Zong, K., Kelemen, P.B., Gao, S., 2008. Geochemistry and magmatic history of eclogites
956 and ultramafic rocks from the Chinese continental scientific drill hole: Subduction and ultrahigh-
957 pressure metamorphism of lower crustal cumulates. Chemical Geology 247, 133-153.
958
959 Locmelis, M., Pearson, N.J., Barnes, S.J., Fiorentini, M.L., 2011. Ruthenium in komatiitic chromite.
960 Geochimica et Cosmochimica Acta 75, 3645-3661.
961
962 Lorand, J.-P., 1989. Are spinel lherzolite xenoliths representative of the abundances of sulphur in
963 the upper mantle? Geochimica et Cosmochimica Acta 54, 1487-1492.
964
965 Lorand, J.-P., Alard, O., Godard, M., 2008. Platinum-group element signatures of the primitive
966 mantle rejuvenated by melt-rock reactions: evidence from Sumail peridotites (Oman Ophiolite).
967 Terra Nova 21, 35-40.
968
969 Lorand, J.-P., Luguet, A., Alard, O., 2008. Platinum-group elements: a new set of key tracers for the
970 Earth's interior. Elements 4, 247-252.
971
972 Lorand, J.-P., Luguet, A., Alard, O., 2012. Platinum-group element systemstics and petrogenetic
973 processing of the continental upper mantle: a review. Lithos 164-167, 2-21.
974
975 Luguet, A., Shirey, S.B., Lorand, J.-P., Horan, M.F., Carlson, R.W., 2007. Residual platinum-group
976 minerals from highly depleted harzburgites of the Lherz massif (France) and their role in HSE
977 fractionation of the mantle. Geochimica et Cosmochimica Acta 71, 3082-3097.
978

979 Maier, W.D., Barnes, S.-J., 2004. Pt/Pd and Pd/Ir ratios in mantle-derived magmas: A possible role
980 for mantle metasomatism. South African Journal of Geology 107, 333-340.
981
982 Maier, W.D., Peltonen, P., McDonald, I., Barnes, S.J., Barnes, S.J., Hatton, C., Viljoen, F., 2012.
983 The concentration of platinum-group elements and gold in southern African and Karelian
984 kimberlite-hosted mantle xenoliths: Implications for the noble metal content of the Earth's mantle.
985 Chemical Geology, 302, 119-135.
986
987 Marchesi, C., Garrido, C.J., Godard, M., Belley, F., Ferré, E., 2009. Migration and accumulation of
988 ultra-depleted subduction-related melts in the Massif du Sud ophiolite (New Caledonia). Chemical
989 Geology 266, 171-186.
990
991 Marchesi, C., Garrido, C.J., Padrón-Navarta, J.A., Sánchez-Vizaíno, V.L., Gómez-Pugnaire, M.T.,
992 2013a. Element mobility from seafloor serpentinisation to high-pressure dehydration of antigorite in
993 subducted serpentinite: Insights from the Cerro del Almirez ultramafic massif (southern Spain).
994 Lithos 178, 128-142.
995
996 Marchesi, C., Garrido, C.J., Harvey, J., González-Jiménez, J.M., Hidas, K., Lorand, J.P., Gervilla,
997 F., 2013b. Platinum-group elements, S, Se and Cu in highly depleted abyssal peridotites from the
998 Mid-Atlantic Ocean Ridge (ODP Hole 1274A): Influence of hydrothermal and magmatic processes.
999 Contributions to Mineralogy and Petrology 166, 1521-1538.
1000
1001 Matsukage, K., Kubo, K., 2003. Chromian spinel during melting experiments of dry peridotite
1002 (KLB-1) at 1.0-2.5 GPa. American Mineralogist 88, 1271-1278.

1003

1004 Momme, P., Tegner, C., Brooks, C.K., Keays, R.R., 2002. The behavious of platinum-group
1005 elements in basalts from the East Greenland rift margin. Contributions to Mineralogy and Petrology
1006 143, 133-153.

1007

1008 Müntener, O., Ulmer, P., 2006. Experimentally derived high-pressure cumulates from hydrous arc
1009 magmas and consequences for the seismic velocity structure of island arc crust. Geophysical
1010 Research Research Letters 33, L21308.

1011

1012 Müntener, O., Kelemen, P.B., Grove, T.L., 2001. The role of H2O during crystallisation of
1013 primitive arc magmas under uppermost mantle conditions and genesis of igneous pyroxenites: an
1014 experimental study. Contributions to Mineralogy and Petrology 141, 643-658.

1015

1016 Næraa, T., Scherstén, A., Rosing, M.T., Kemp, A.I.S., Hoffmann, J.E., Kokfelt, T.F., Whitehouse,
1017 M.J., 2012. Hafnium isotope evidence for a transition in the dynamics of continental growth 3.2 Gyr
1018 ago. Nature 485, 627-630.

1019

1020 Nielsen, T.F.D., 1981. The ultramafic cumulates series, Gardiner Complex, East Greenland –
1021 Cumulates in a shallow level magma chamber of a nephelinitic volcano. Contributions to
1022 Mineralogy and Petrology 76, 60-72.

1023

1024 Niu, Y., 2004. Bulk-rock major and trace element compositions of abyssal peridotites: implications
1025 for mantle melting, melt extraction and post-melting processes beneath mid-ocean ridges. Journal of
1026 petrology 45, 2423-2458.

Nutman, A.P., Kalsbeek, F., 1994. A minimum age of 2944 +/- 7 Ma for the Tartoq Group, South-West Greenland. Rapport Grønlands Geologiske Undersøgelse 161, 35-38.

Nutman, A.P., Friend, C.R.L., Barker, S.L.L., McGregor, V.R., 2004. Inventory and assessment of Palaeoarchaean gneiss terrains and detritial zircons in southern West Greenland. Precambrian Research 135, 281-314.

O'Hanley, D.S., 1996. Serpentinites: Records of tectonic and petrological history. New York: Oxford University Press, 277 pp.

Ordóñez-Calderón, J.C., Polat, A., Fryer, B.J., Gagnon, J.E., Raith, J.G., Appel, P.W.U., 2008. Evidence for HFSE and REE mobility during calc-silicate metasomatism, Mesoarchean (~ 3075Ma) Ivisaartoq greenstone belt, southern West Greenland. Precambrian Research 161, 317-340.

Ordóñez-Calderón, J.C., Polat, A., Fryer, B.J., Gagnon, J.E., 2011. Field and geochemical characteristics of Mesoarchean to Neoarchean volcanic rocks in the Storø greenstone belt, SW Greenland: Evidence for accretion of intra-oceanic volcanic arcs. Precambrian Research 184, 24-42.

Pagé, P., Barnes, S.J., 2009. Using trace elements in chromites to constrain the origin of podiform chromitites in the Thetford Mines ophiolite, Québec, Canada. Economic Geology 104, 997-1018.

1050 Palme, H., and O'Neill, H.C., 2003. Compositional estimates of mantle composition, In: Carlson,
1051 R.W. (Ed.), The Mantle and Core, v. 2, Oxford, UK, Elsevier-Pergamon, p. 1-38.
1052
1053 Parkinson, I.J., Pearce, J.A., 1998. Peridotites from the Izu–Bonin–Mariana forearc (ODP Leg 125):
1054 evidence for mantle melting and melt–mantle interaction in a supra-subduction zone setting. Journal
1055 of Petrology 39, 1577-1618.
1056
1057 Paulick, H., Bach, W., Godard, M., De Hoog, J.C.M., Suhr, G., Harvey, J., 2006. Geochemistry of
1058 abyssal peridotites (Mid-Atlantic Ridge, 15°20'N, ODP Leg 209): Implications for for fluid/rock
1059 interaction in slow spreading environments. Chemical geology 234, 179-210.
1060
1061 Petersen, J.S., 1992. Nuuluk-Iterlak gold and massive-sulfide project, Taartoq Archaean greenstone
1062 belt, SW Greenland. Field report, Nunaoil A/S, 164 pp.
1063
1064 Peucker-Ehrenbrink, B., Hanghøj, K., Atwood, T., Kelemen, P.B., 2012. Rhenium-osmium isotope
1065 systematics and platinum group element concentrations in oceanic crust. Geology 40, 199-202.
1066
1067 Pirard, C., Hermann, J., O'Neill, H.S.C., 2013. Petrology and Geochemistry of the Crust–Mantle
1068 Boundary in a Nascent Arc, Massif du Sud Ophiolite, New Caledonia, SW Pacific. Journal of
1069 Petrology (in press).
1070
1071 Polat, A., Hofmann, A.W., 2003. Alteration and geochemical patterns in the 3.7-3.8 Ga Isua
1072 greenstone belt, West Greenland. Precambrian Research 126, 197–218.
1073

1074 Polat, A., Appel, P.W.U., Fryer, B.J., 2011. An overview of the geochemistry of Eoarchean to
1075 Mesoarchean ultramafic to mafic volcanic rocks, SW Greenland: Implication for mantle depletion
1076 and petrogenetic processes at subduction zones in the early Earth. Gondwana Research 20, 255-283.
1077
1078 Rehkämper, M., Halliday, A.N., Barfod, D., Fitton, J.G., Dawson, J.B., 1997. Platinum-group
1079 element abundance patterns in different mantle environments. Science 278, 1595-1598.
1080
1081 Rollinson, H., 2002. The metamorphic history of the Isua greenstone belt, West Greenland.
1082 Geological Society, London, Special Publications 199, 329-350.
1083
1084 Rollinson, H., 2007. Recognising early Archaean mantle: a reappraisal. Contributions to
1085 Mineralogy and Petrology 154, 241-252.
1086
1087 Säntti, J., Kontinen, A., Sorjonen-Ward, P., Johanson, B., Pakkanen, L., 2006. Metamorphism and
1088 chromite in serpentinized and carbonate-silica-altered peridotites of the Paleoproterozoic
1089 Outokumpu-Jormua Ophiolite Belt, Eastern Finland. International Geology Review 48, 494-546.
1090
1091 Savard, D., Barnes, S-J., Meisel, T., 2010. Comparison between Ni-fire assay Te co-percipitation
1092 and isotope dilution with high pressure asher acid digestion for the determination of platinum-group
1093 elements, rhenium and gold. Geostandards and Geoanalytical Research 34, 281-291.
1094
1095 Shirey, S.B., Walker, R.J., 1998. The Re-Os isotope system in cosmochemistry and high-
1096 temperature geochemistry. Annual Review of Earth and Planetary Sciences 26, 423-500.
1097

1098 Shirey, S.B., Richardson, S.H., 2011. Start of the Wilson cycle at 3 Ga shown by diamonds from
1099 subcontinental mantle. Science 333, 434-436.
1100
1101 Snow, J.E., Dick, H.J.B., 1995. Pervasive magnesium loss by marine weathering of peridotite.
1102 Geochimica et Cosmochimica Acta 59, 4219-4235.
1103
1104 Suárez, S., Prichard, H.M., Velasco, F., Fisher, P.C., McDonald, I., 2010. Alteration of platinum-
1105 group minerals and dispersion of platinum-group elements during progressive weathering of the
1106 Aguablanca Ni–Cu deposit, SW Spain. Mineralium Deposita 45, 331-350.
1107
1108 Szilas, K., Næraa, T., Scherstén, A., Stendal, H., Frei, R., van Hinsberg, V.J., Kokfelt, T.F., Rosing,
1109 M.T., 2012a. Origin of Mesoarchaean arc-related rocks with boninite/komatiite affinities from
1110 southern West Greenland. Lithos, 144, 24-39.
1111
1112 Szilas, K., Hoffmann, J.E., Scherstén, A., Rosing, M.T., Kokfelt, T.F., Windley, B.F., Van
1113 Hinsberg, V.J., Næraa, T., Keulen, N., Frei, R., Münker, C., 2012b. Complex calc-alkaline
1114 volcanism recorded in Mesoarchaean supracrustal belts north of Frederikshåb Isblink, southern
1115 West Greenland: implications for subduction zone processes in the early Earth. Precambrian
1116 Research, 208-211, 90-123.
1117
1118 Szilas, K., van Hinsberg, J., Kisters, A.F.M., J. Hoffmann, E., Kokfelt, T.F., Scherstén, A.,
1119 Windley, B.F., Münker, C., 2013a. Remnants of arc-related Mesoarchaean oceanic crust in the
1120 Tartoq Group, SW Greenland. Gondwana Research 23, 436-451.
1121

1122 Szilas, K., Hoffmann, J.E., Scherstén, A., Kokfelt, T.F, Münker, C., 2013b. Archaean andesite
1123 petrogenesis: insights from the Grædefjord Supracrustal Belt, SW Greenland. Precambrian
1124 Research 236, 1-15.
1125
1126 Szilas, K., Van Gool, J.A.M., Scherstén, A., Frei, R. The Meso- to Neoarchaean 'Storø Supracrustal
1127 Belt', Nuuk region, southern West Greenland: a mafic arc-related basin with continent-derived
1128 sedimentation. Precambrian Research (**in press**).
1129
1130 Szilas, K., Garde, A.A. 2013. Mesoarchaean aluminous rocks at Storø, southern West Greenland:
1131 new age data and evidence of premetamorphic seafloor weathering of basalts. Chemical Geology
1132 354, 124–138.
1133
1134 Takazawa, E., Frey, F.A., Shimizu, N., Obata, M., Bodinier, J.L., 1992. Geochemical evidence for
1135 melt migration and reaction in the upper mantle. Nature 359, 55-58.
1136
1137 Tatsumi, T., 1981. Melting experiments on a high-magnesian andesite. Earth and Planetary Science
1138 Letters 54, 357-365.
1139
1140 Thakurta, J., Ripley, E.M., Li, C., 2008. Geochemical constraints on the origin of sulfide
1141 mineralization in the Duke Island Complex, southeastern Alaska. Geochemistry Geophysics
1142 Geosystems 9, Q07003.
1143
1144 Umino, S., Kushiro, I., 1989. Experimental studies on boninite petrogenesis. In: Crawford, A.J.
1145 (Ed.), Boninites and related rocks. Unwin Hyman, London, pp. 89-111.

Van Hinsberg, V.J., Szilas, K., Kisters, A.F.M., 2010. The Tartoq Group, SW Greenland: Mineralogy, textures and a preliminary metamorphic to hydrothermal history. Danmarks og Grønlands Geologiske Undersøgelse Rapport 2010/120, 52 pp.

Wang, J., Hattori, K.H., Stern, C., 2008. Metasomatic origin of garnet orthopyroxenites in the sub-continental lithospheric mantle underlying Pali Aike volcanic field, southern South America. Mineralogy and Petrology 94, 243-58.

Windley, B.F., 1991. Early Proterozoic collision tectonics, and rapakivi granites as intrusions in an extensional thrust-thickened crust: the Ketilidian orogen, South Greenland. Tectonophysics 195, 1-10.

Windley, B.F., Garde, A.A., 2009. Arc-generated blocks with crustal sections in the North Atlantic craton of West Greenland: crustal growth in the Archean with modern analogues. Earth Science Reviews 93, 1-30.

Wittig, N., Pearson, D.G., Webb, M., Ottley, C.J., Irvine, G.J., Kopylova, M., Jensen, S.M., Nowell, G.M., 2008. Origin of cratonic lithospheric mantle roots: A geochemical study of peridotites from the North Atlantic Craton, West Greenland. Earth and Planetary Science Letters 274, 24-33.

Wittig, N., Webb, M., Pearson, D.G., Dale, C.W., Ottley, C.J., Hutchison, M., Jensen, S.M., Luguet, A., 2010. Formation of the North Atlantic Craton: Timing and mechanisms constrained

from Re–Os isotope and PGE data of peridotite xenoliths from SW Greenland. Chemical Geology 276, 166-187.

Wood, B.J., Turner, S.P., 2009. Origin of primitive high-Mg andesite: Constraints from natural examples and experiments. Earth and Planetary Science Letters 283, 59-66.

Woodland, S.J., Pearson, D.G., Thirlwall, M.F., 2002. A platinum group element and Re-Os isotope investigation of siderophile element recycling in subduction zones: comparison of Grenada, Lesser Antilles Arc, and the Izu-Bonin Arc. Journal of Petrology 43, 171-198.

Xie, Z., Hattori, K., Wang, J., 2013. Origins of ultramafic rocks in the Sulu Ultrahigh-pressure Terrane, Eastern China. Lithos 178, 158-170.

Figure captions

Figure 1. Geological map of the Mesoarchaean Tartoq Group (dark green) and the Palaeoproterozoic Ketilidian supracrustal rocks (light green), which unconformably overlie the former. Based on mapping by GEUS.

Figure 2. Detailed geological maps of the serpentinite localities of the Tartoq Group. Overview maps modified after van Hinsberg et al. (2010). Detailed maps based on 2010 mapping by the authors. Figure 2d is a close-up of the box on the Iterlak map (Fig. 2a). Figure 2e is a close-up of the box on the Amitsuarsua map (Fig. 2b).

Figure 3. Microphotographs of the Tartoq Group serpentinites. a) Typical serpentinite showing distinct boxwork/mesh texture. Serpentine patches seem to pseudomorph original minerals (olivine and/or orthopyroxene) and are surrounded by a mesh of chromite. Note the alignment of the elongated mineral-pseudomorphs. b) Serpentinite from Bikuben, showing an example of the characteristic veined texture type, containing abundant magnetite. The width of both microphotographs is 5 mm.

Figure 4. Element variation of the Tartoq Group serpentinites plotted against MgO. Note the general lack of correlations and the tight compositional ranges. Major elements are in wt.% and trace elements in ppm. Although there are no obvious correlations in the major element variation diagrams (Fig. 4), there is a tendency for elevated Cr and V in the low-Ir group of serpentinites, which are commonly veined by magnetite and chromite (see **Section 5.2**).

Figure 5. Primitive mantle-normalised trace element diagram for the Tartoq Group serpentinites. There are no significant differences between these two groups and both are generally parallel with the Tartoq Group mafic volcanic sequence (Szilas et al., 2013a). Primitive mantle abundances are from Palme and O'Neill (2003).

Figure 6. Chondrite-normalised platinum-group element (PGE) patterns for the Tartoq Group serpentinites. Chondrite abundances from Fisher-Gödde et al. (2010). The low-Ir group serpentinites have distinctly positive Ru anomalies, which are possibly related to accumulation of chromite. The high-Ir serpentinites have flattish PGE patterns, but also negative Pt anomalies.

Figure 7. In situ laser ablation element patterns for the Tartoq Group spinels. Normalised to chromites from MORB (Pagé and Barnes, 2009). Circles represent chromite core analyses, triangles are from rims and squares are from massive grains. The shaded area marks the total range of the samples.

Figure 8. Comparison between the Tartoq Group and the Kohistan arc complex. Data of the Kohistan arc complex from Jagoutz and Schmidt (2012). Note the broad overlap of the ultramafic lithologies, which covers the same ranges in compatible elements and in particular the similar range in FeOt, which is a diagnostic feature of these ultramafic rocks.

Figure 9. Comparison between the Tartoq Group assemblage and the calculated liquid evolution and corresponding bulk cumulates. Oxygen fugacity is buffered at QFM and the pressure is constant at 2 Kb with an initial H_2O content of 0.5 wt.%. The initial cumulate is dominated by olivine (98%) and chromite (2%), which are joined by plagioclase below 1180°C (the most evolved cumulates are not shown).

Supplementary online material

Appendix A: Detailed methods description

Appendix B: Supplementary diagrams

Supplementary Table 1. Bulk-rock major and trace element data and normative mineralogy.

Supplementary Table 2. Bulk-rock platinum-group element data.

Supplementary Table 3. Electron microprobe data.

Supplementary Table 4. In situ laser ablation ICP-MS spinel data

Supplementary Table 5. Bulk-rock Re-Os isotope data.

Figure 1

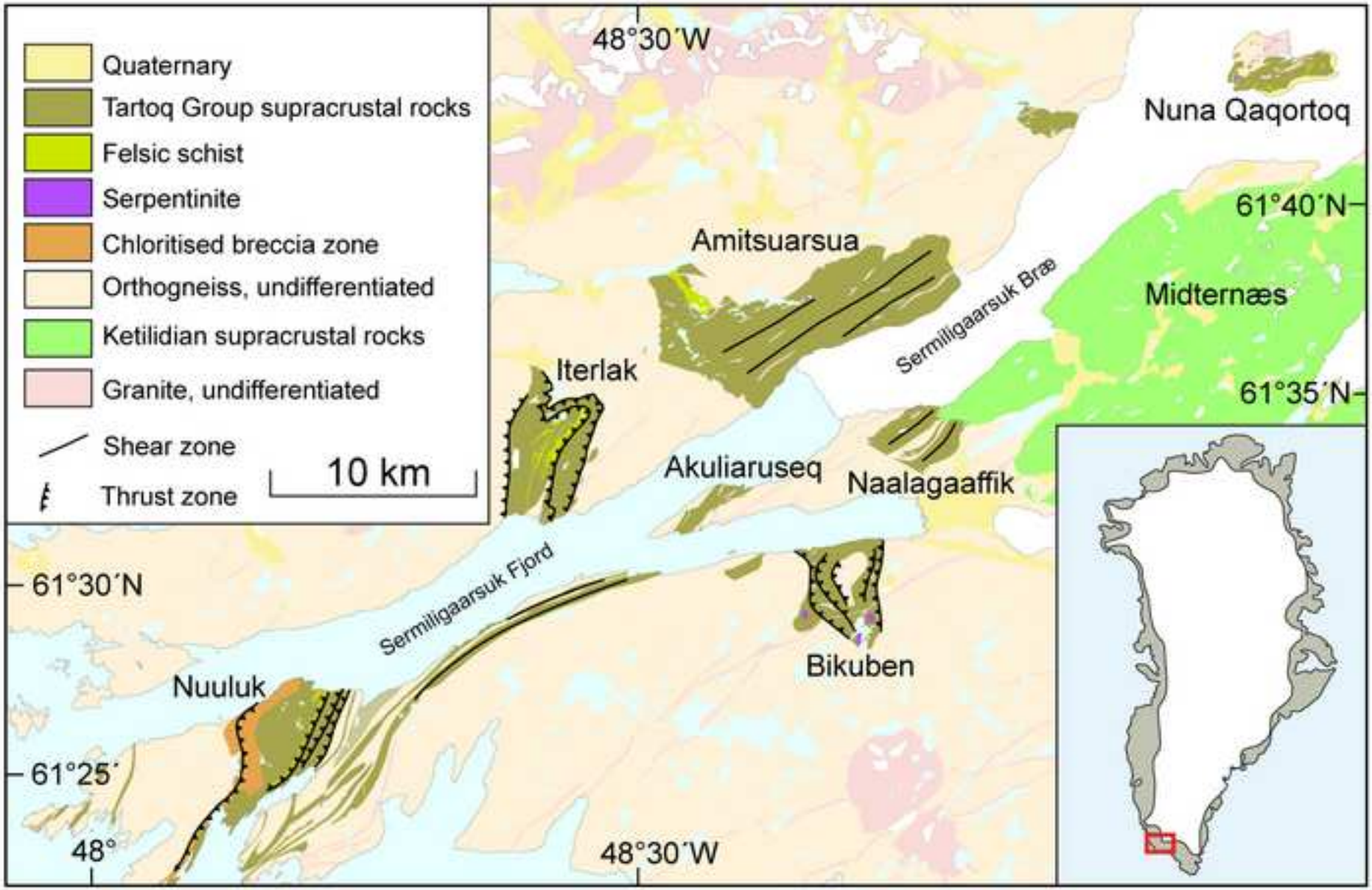
Quaternary
Tartoq Group supracrustal rocks
Felsic schist
Serpentinite
Chloritised breccia zone
Orthogneiss, undifferentiated
Ketilidian supracrustal rocks
Granite, undifferentiated
Shear zone
Thrust zone
10 km
48°30´W
Nuna Qaqortoq
61°40´N
Amitsuarsua
Sermiligaarsuk Bræ
Midternæs
Iterlak
61°35´N
Akuliaruseq
Naalagaaffik
61°30´N
Sermiligaarsuk Fjord
Bikuben
Nuuluk
61°25´
48°
48°30´W

Figure 2

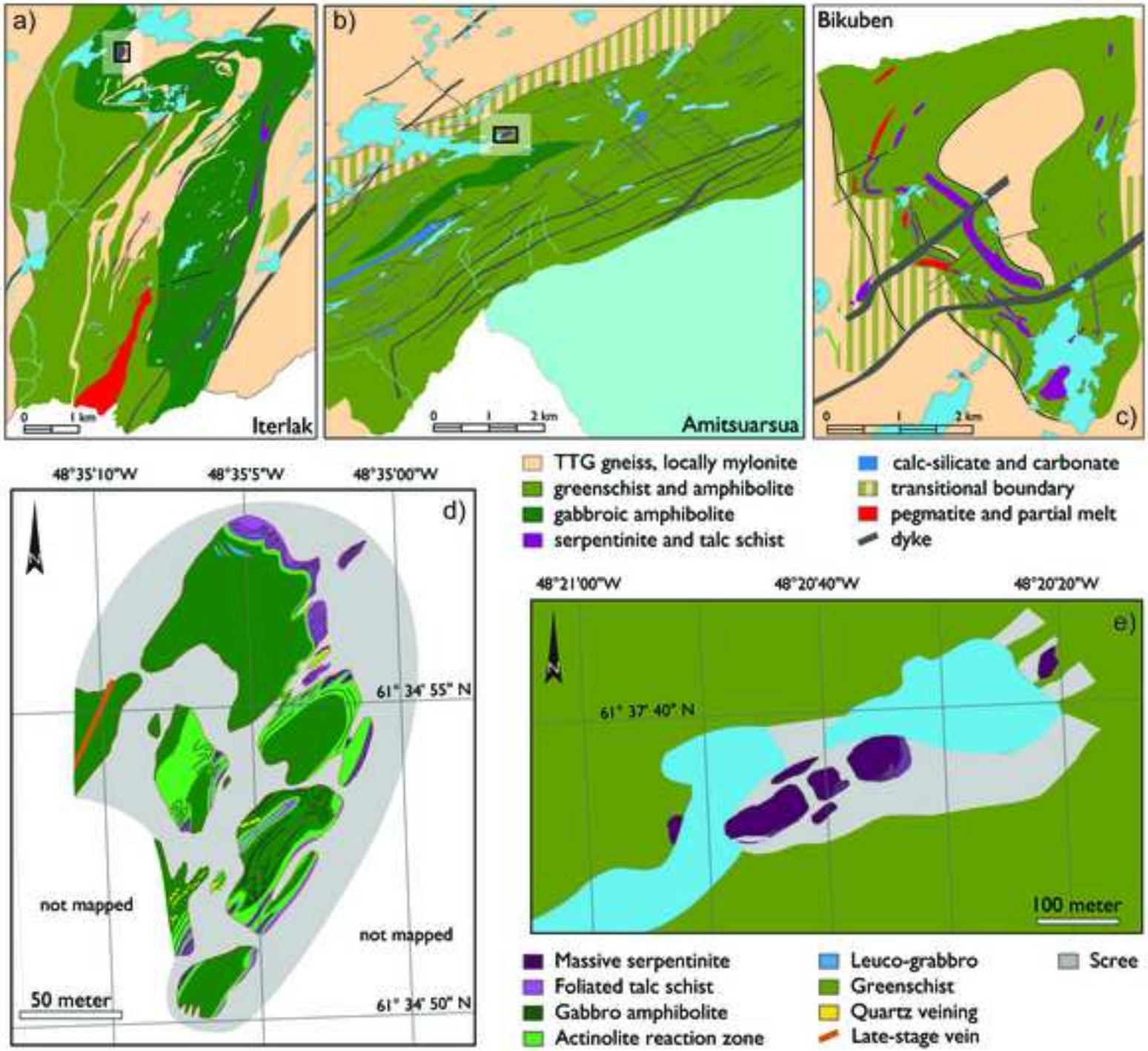
a)
Iterlak
0
1 km
b)
Amitsuarsua
0
1
2 km
Bikuben
c)
0
1
2 km
TTG gneiss, locally mylonite
greenschist and amphibolite
gabbroic amphibolite
serpentinite and talc schist
calc-silicate and carbonate
transitional boundary
pegmatite and partial melt
dyke
48°35'10"W
48°35'5"W
48°35'00"W
d)
61° 34' 55" N
61° 34' 50" N
not mapped
not mapped
50 meter
48°21'00"W
48°20'40"W
48°20'20"W
e)
61° 37' 40" N
100 meter
Massive serpentinite
Foliated talc schist
Gabbro amphibolite
Actinolite reaction zone
Leuco-grabbro
Greenschist
Quartz veining
Late-stage vein
Scree

Figure 3

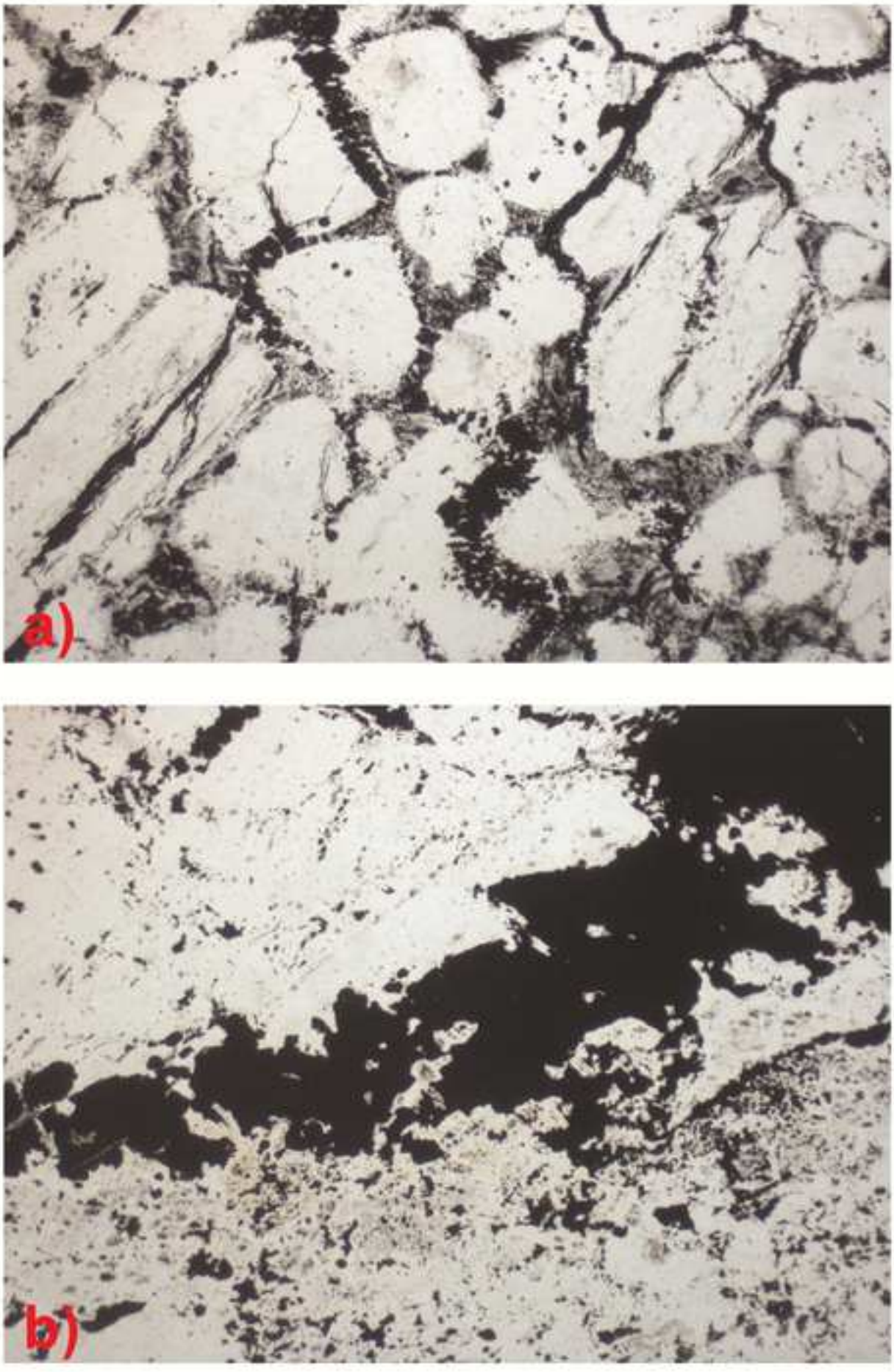

Figure 4

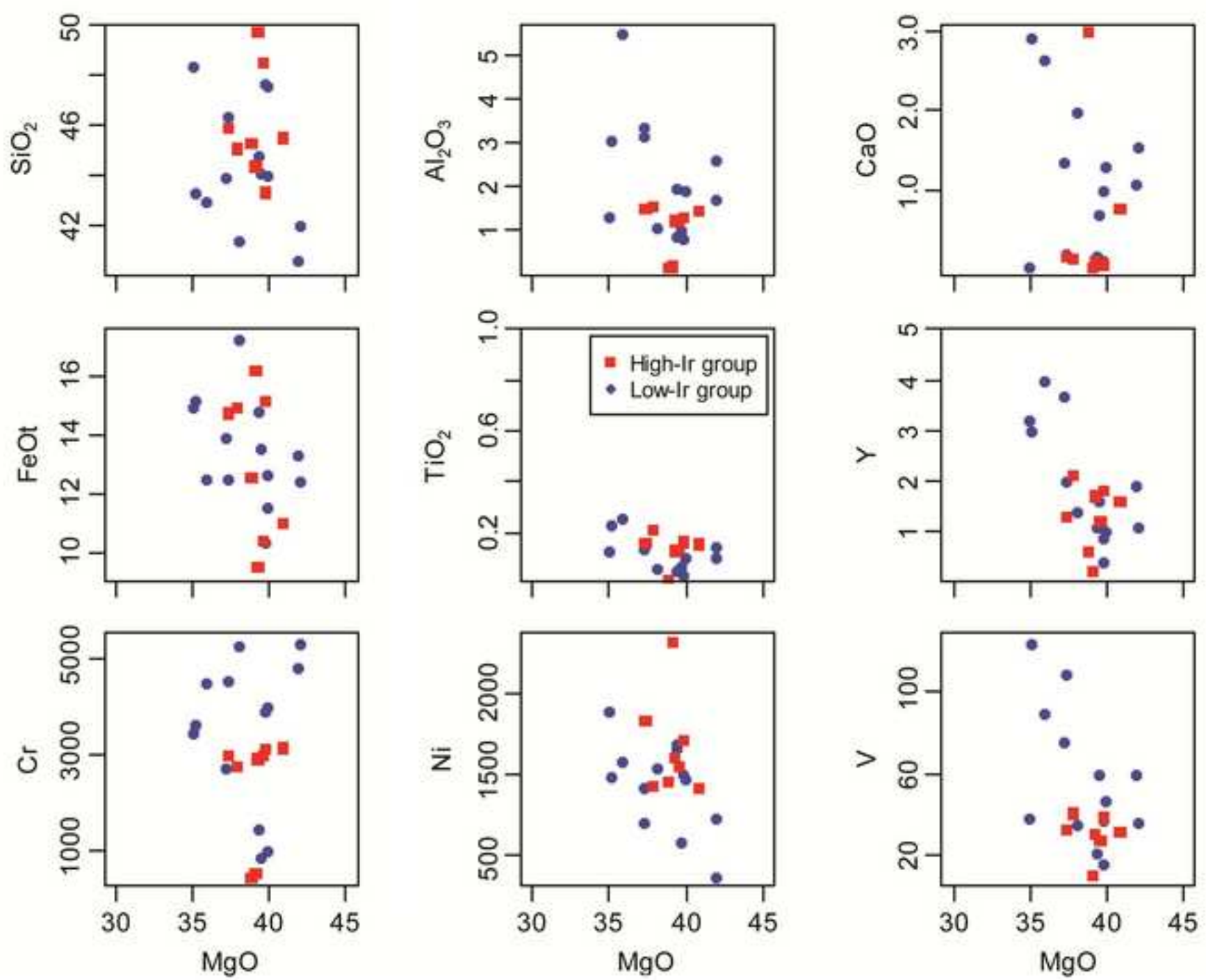
SiO2
42
46
50
Al2O3
1
2
3
4
5
CaO
1.0
2.0
3.0
FeOt
10
12
14
16
TiO2
0.2
0.6
1.0
High-Ir group
Low-Ir group
Y
1
2
3
4
5
Cr
1000
3000
5000
Ni
500
1500
2000
V
20
60
100
30
35
40
45
MgO

Figure 5

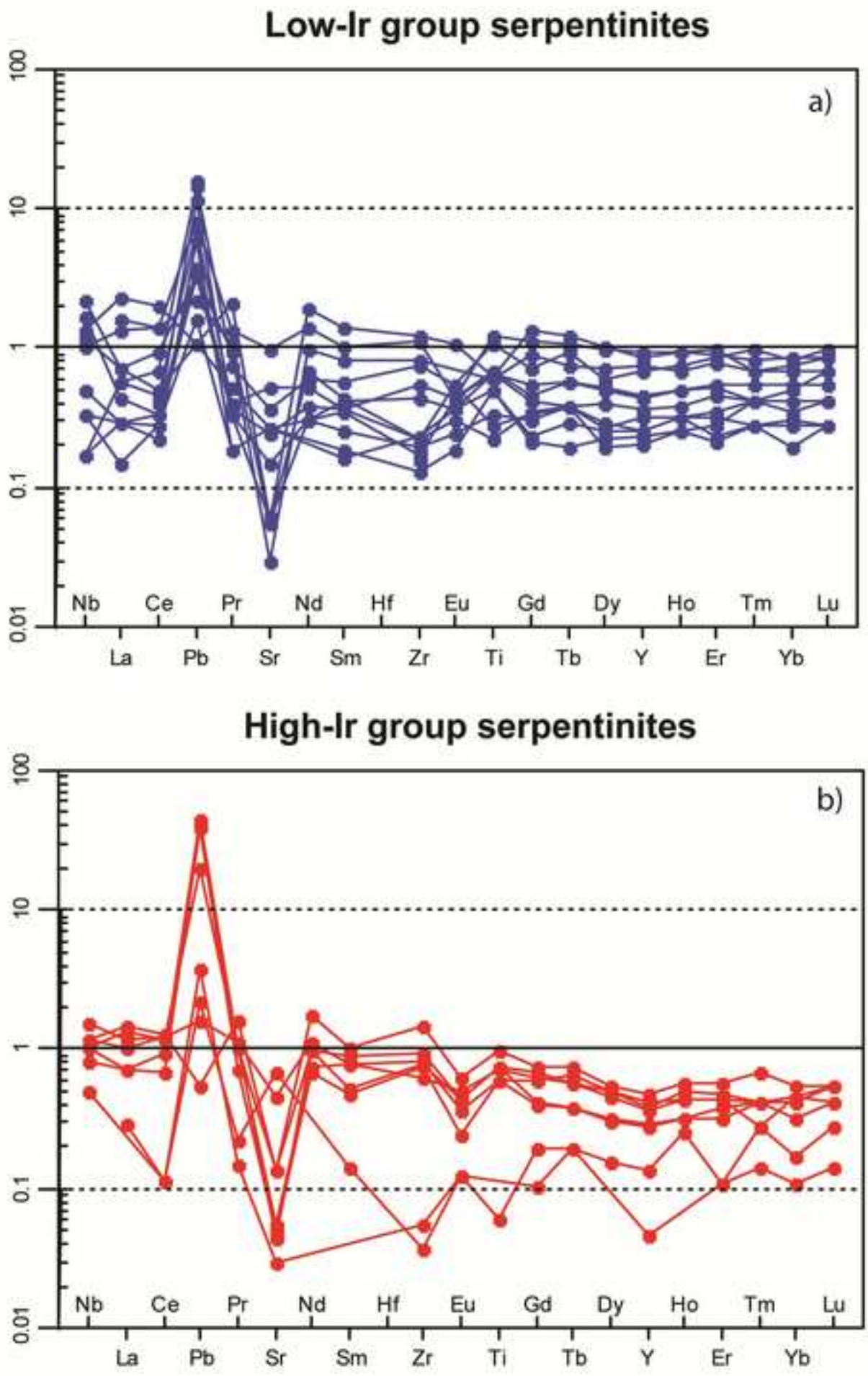
Low-Ir group serpentinites
a)
100
10
1
0.1
0.01
Nb Ce Pr Nd Hf Eu Gd Dy Ho Tm Lu
La Pb Sr Sm Zr Ti Tb Y Er Yb
High-Ir group serpentinites
b)
100
10
1
0.1
0.01
Nb Ce Pr Nd Hf Eu Gd Dy Ho Tm Lu
La Pb Sr Sm Zr Ti Tb Y Er Yb

Figure 6

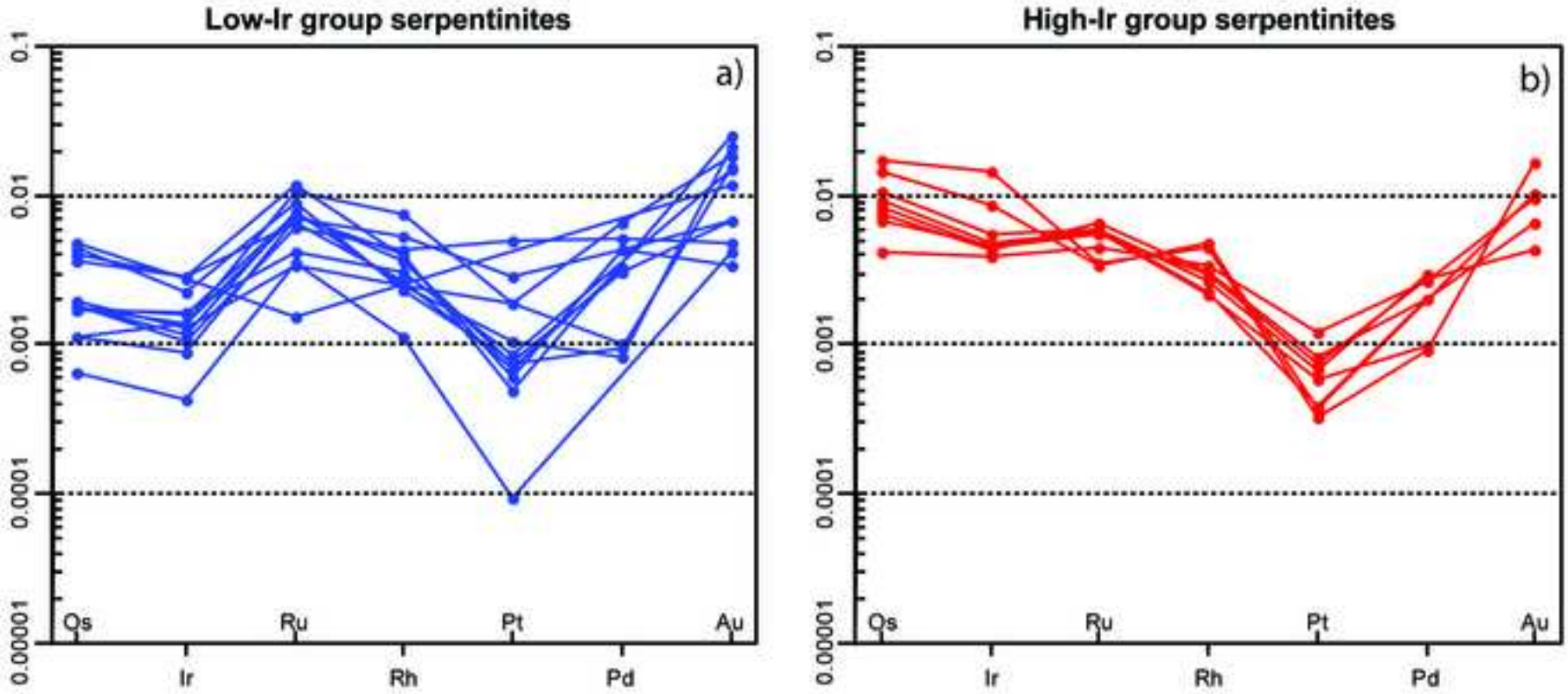
Low-Ir group serpentinites
a)
0.1
0.01
0.001
0.0001
0.00001
Os
Ir
Ru
Rh
Pt
Pd
Au
High-Ir group serpentinites
b)
0.1
0.01
0.001
0.0001
0.00001
Os
Ir
Ru
Rh
Pt
Pd
Au

Figure 7

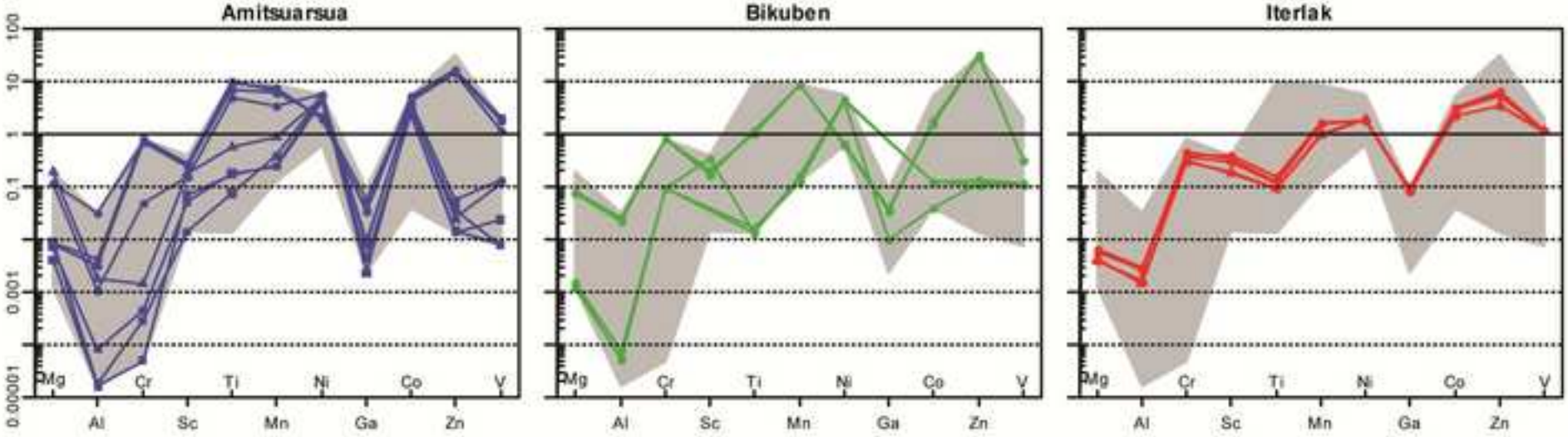
Amitsuarsua
Bikuben
Iterlak
100
10
1
0.1
0.001
0.00001
Mg
Cr
Ti
Ni
Co
V
Al
Sc
Mn
Ga
Zn

Figure 8

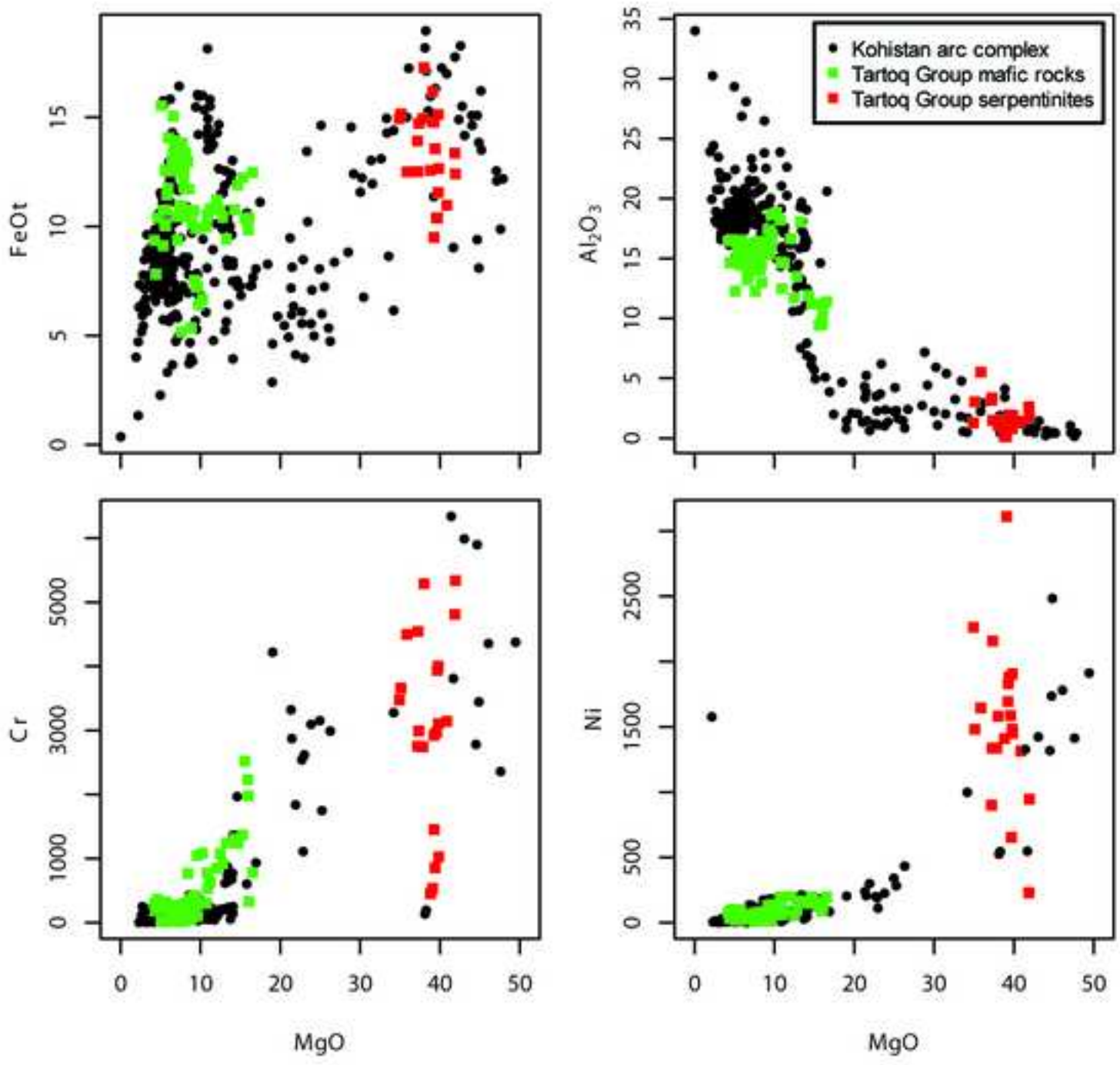
Kohistan arc complex
Tartoq Group mafic rocks
Tartoq Group serpentinites
FeOt
Al_2O_3
Cr
Ni
MgO
MgO

Figure 9

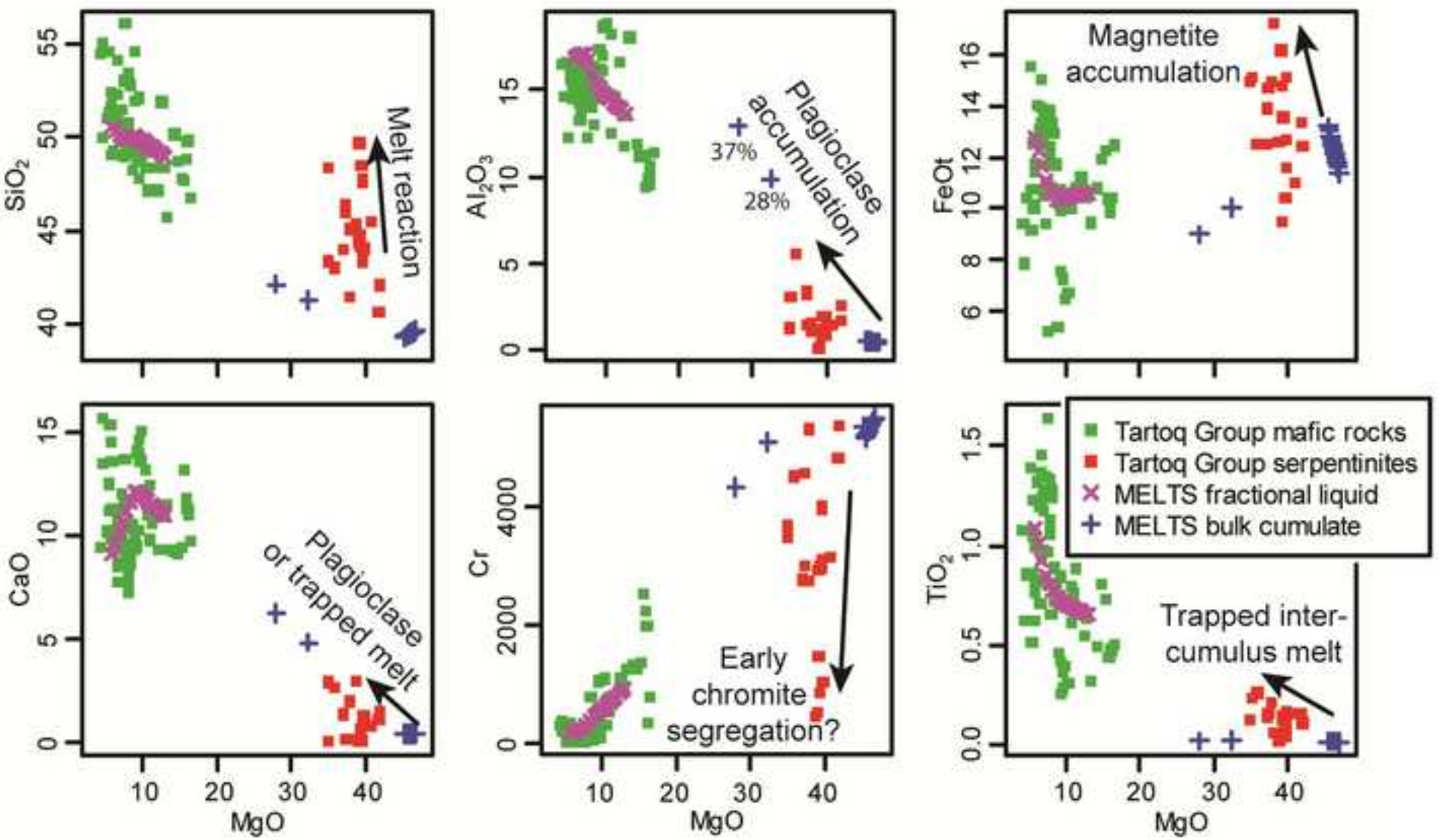
SiO2
Melt reaction
Al2O3
37%
28%
Plagioclase accumulation
FeOt
Magnetite accumulation
CaO
Plagioclase or trapped melt
Cr
Early chromite segregation?
TiO2
Trapped inter-cumulus melt
MgO
Tartoq Group mafic rocks
Tartoq Group serpentinites
MELTS fractional liquid
MELTS bulk cumulate